AN ANALYSIS OF CONVECTIVE HEAT TRANSFER IN TUBES

A Thesis

Presented to

the Faculty of Graduate Studies and Research

University of Manitoba

In Partial Fulfillment

of the Requirements for the Degree

Master of Science in Mechanical Engineering

---

by

Germain Joseph Maguet

April 1965

ACKNOWLEDGEMENTS

I with to thank Professor R.E. Chant, Chairman of the Department of Mechanical Engineering, for his excellent guidance throughout the preparation of this thesis.

Special gratitude is offered to Messrs. G. Babiy and O. Tonn, whose suggestions on the construction of the test equipment were greatly appreciated, and to Messrs. D. Gillies and H. Weiss who helped with the construction of the test rig and the accumulation of test data.

A great deal of appreciation is extended to: my employer, W.L. Wardrop & Associates, for permitting the use of their typing and drafting facilities and for special privileges obtained during this undertaking; my wife Denise, for her encouragement and helpfulness throughout this project; Mr. Don Gruhn who helped in the presentation of drawings and clarified many important points; and to Mr. John T. Berry, for his constructive comments.

Finally, I am grateful to all others who have devoted themselves immensely in making the presentation of this thesis possible.

AN ANALYSIS OF CONVECTIVE HEAT TRANSFER IN TUBES

by

Germain Joseph Maguet

April 1965

ABSTRACT

The convective heat transfer inside a tube has been investigated for conditions varying from laminar to turbulent flow; over a Reynolds Number range from 1,164 to 135,900. Thirty-six tests were carried out in an apparatus which consisted of an inner pipe surrounded by an outer pipe through which water was passed for cooling purposes. The experimental work for this thesis was carried out during the 1958 - 59 academic year.

The Appendix contains the tabulated results and plotted curves which were based on a surface coefficient h_w for water in the annulus of 500 BTU/hr/ft^2/^{o}F. It was finally established that the value of h_w should have been in the order of 50 BTU/hr/ft^2/^{o}F. When the test results were replotted based on the corrected h_w they were found to agree closely with that of other observers.

Results for the average heat transfer coefficient at laminar flow conditions were inconclusive due to the small number of tests carried out at low flow conditions: At turbulent flow conditions; the results obtained by Sieder and Tate (Reference 1 in the thesis).

The local heat transfer coefficient along the tube was found to be large at the tube inlet, decreasing rapidly in the direction of flow for a length of five diameters, then decreasing slowly over the remaining length.

TABLE OF CONTENTS

LIST OF FIGURES

LIST OF TABLES

FIGURE PAGE

NOMENCLATURE

LATIN LETTERS

A	area
C	constant
C_p	specific heat at constant pressure
C_f	skin friction coefficient
C_h	heat transfer factor
D	diameter or characteristic length
E	ratio of momentum to heat diffusivity
F	degrees Fahrenheit, also Martinelli factor
f	friction coefficient for flow through a tube
G	mass velocity
g	acceleration of gravity
h	heat transfer coefficient
h_x	local heat transfer coefficient
h_a, h_m	average or mean heat transfer coefficient
J	mechanical equivalent of heat, heat transfer factor
K	thermal conductivity
ln	natural logarithm
L	length
L_c	critical length
Q	heat flow per unit time
r	radius of pipe

R	degrees Rankine
t	temperature
t_s, t_w	surface or wall temperature
t_b, tB	bulk temperature
ta, t_m	average or mean temperature
t_c	temperature at centre of pipe
t_∞	main stream temperature
u, v	velocity components
V_m	mean velocity
V_∞	free stream velocity
U	overall heat transfer coefficient
V	velocity
W	flow rate, weight density
x	distance from tube inlet
x, y, z	coordinate axes

GREEK LETTERS

α (alpha)	thermal diffusivity
Δ (Delta)	incremental or difference sign
	Δ t, temperature difference
δ (delta)	boundary layer thickness
	δ_{tu}, turbulent boundary layer thickness
	δ_b, laminar sublayer thickness

ϵ (epsilon) ϵ_m, eddy diffusivity for momentum

ϵ_q, eddy diffusivity for heat

μ (mu) dynamic viscosity

μ_B, at bulk fluid temperature

μ_f, at film temperature

ν (nu) kinematic viscosity

ρ (rho) density

σ (sigma) shear stress

τ (tau) transmissivity

DIMENSIONLESS NUMBERS

N_{Re} = Reynolds Number

N_{Pr} = Prandtl Number

N_{Nu} = Nusselt Number

N_{Pe} = Péclet Number

N_{St} = Stanton Number

N_{Gz} = Graetz Number

INTRODUCTION

The science of heat transfer which deals with the rates of exchange of heat between bodies of different temperatures is very complex. Theoretical analyses are still limited and a great deal of experimentation and research is still necessary to fully evaluate all aspects of a particular problem.

Tubes and pipes are frequently used for the transmission of liquids and gases from one location to another and as heat exchanger surfaces, consequently, the heat transfer characteristics for tubes is of great importance to the designer of heat exchange equipment. The effect of the tube entrance conditions on the overall heat transfer characteristic along the tube length is an important phase in the study of heat transfer in tubes. In tubular heat exchangers designed to transfer large quantities of heat from low viscosity fluids flowing in tubes, the tubes may be of such a length and turbulent flow develop so quickly that the entrance effect is negligible. For highly viscous fluids such as oil, the tube length necessary for the full development of the hydrodynamic and thermal boundary layers may be so long that it may never be attained in a particular heat exchanger.

This thesis is an analysis of heat transfer in tubes substantiated by experimental work to determine the local and average

heat transfer coefficients when using air as the flowing medium. The development of the hydrodynamic and thermal boundary layers in tubes is analysed to determine the relationship between the two.

The local heat transfer coefficient varies along the tube from a high value at the inlet, to a constant value after the flow has become fully developed. The average heat transfer coefficient over any portion of the tube likewise decreases in the direction of flow.

The hydrodynamic boundary layer becomes fully developed at Reynolds Numbers, based on tube diameter, between 2,500 and 3,500 depending on the surface conditions and tube length to diameter ratio. The development of the thermal boundary layer is related to the hydrodynamic layer but the relationship is dependent upon the heat flux and the thermal properties of the fluid.

PART ONE

THEORETICAL AND EMPIRICAL ANALYSES

THEORETICAL ANALYSES

MODES OF HEAT TRANSFER

The theory of heat transfer may be subdivided into three main categories, each of which represents a method by which heat is transferred.

The three methods are commonly referred to as: radiation, conduction and convection. As the net heat transfer in most applications occurs by a combination of two or three of these methods, a brief description of each method will be made here, however, the body of the thesis will deal only with the convective method of heat transfer.

Radiation consists of energy transfer from one body to another by the flow of electromagnetic waves.

Conduction Jakob[1] has two definitions for conduction.

Considered from an atomistic viewpoint, conduction is due to the elastic impacts of molecules in gases, to longitudinal oscillations in solid nonconductors of electricity and to the motion of electrons in metals.

Considered from a phenomenological point of view, it means the exchange of heat between contiguous bodies or parts of a body which are at a different temperature.

The following fundamental conduction equation is attributed

to Fourier[2]:

$$Q = -KA \ dt/dx \quad \ldots\ldots (1)$$

where K = thermal conductivity - BTU/hr/ft/°F

A = area - ft^2

dt/dx = temperature gradient in direction of flow

dt = temperature differential in length dx.

The thermal conductivity "K" is a property of the substance, which varies with temperature for a given medium. In most gases, liquids and homogeneous solids, "K" varies approximately as a linear relation with temperature over a moderate temperature range.

Convection[2] is the transfer of energy by actual physical movement, from one location to another of a substance in which energy is stored. It follows, that any method of increasing the rate of mixing will correspondingly increase the rate of convective heat transfer. The mixing may occur due to free convection as hot air rising in a room, or, it may be forced by causing a fluid to flow over a surface or through a tube.

Heat flow by convection from one medium to another can be determined from the following relation developed by Newton[2]:

$$Q = hA\Delta T \quad \ldots\ldots (2)$$

where ΔT = Difference in temperature between the medium and the surface - ^oF

A = Area of the surface - ft^2

h = Convective heat transfer coefficient $BTU/hr/ft^2/^oF$ which is described in the next section.

CONVECTIVE HEAT TRANSFER COEFFICIENT

Newton's law of cooling, represented by the equation:

$$Q = hA\,(t_{surface} - t_{fluid}) \quad \ldots\ldots (3)$$

is useful in defining "h" as a measure of the convective capacity of the flowing fluid. Noting that the units for "h" are $BTU/hr/ft^2/^oF$ it can be seen that they differ from units of "K" only by a length factor.

Re-writing the basic conduction equation (1) as $Q = KA\,\frac{t_s - t_\infty}{L}$ where $t_s - t_\infty$ is the temperature differential in length "L" and, comparing it to Newton's cooling law, Equation (4) points out the similarity between "h" and "K".

$$Q = hA\,(t_s - t_\infty) = KA\,\frac{t_s - t_\infty}{L} \quad \text{.....(4)}$$

where t_s = surface temperature - ^oF

t_∞ = fluid temperature ^oF at distance "L" from the surface

K = thermal conductivity of the fluid - BTU/hr/ft/^oF

It is apparent that if an appropriate value of "L" were used, the heat tranfer could be considered as occurring by conduction with "h" equal to K/L. This points out that the heat flow through a very thin layer of fluid near a wall occurs by conduction. It is difficult to determine the thickness of this layer. For the wall shown in Figure 1, having a thermal boundary layer " δ ", the slope of the temperature profile in the fluid at the wall is $(dt/dx)_s$, then:

$$Q = hA\,(t_s - t_\infty) = -KA\,(dt/dx)_s \quad \text{.....(5)}$$

therefore:

$$h = \frac{-K(dt/dx)_s}{t_s - t_\infty} \quad \text{.....(6)}$$

Then, for constant t_s and t_∞ , h is a function of $(dt/dx)_s$, which is the slope of the temperature gradient at the surface.

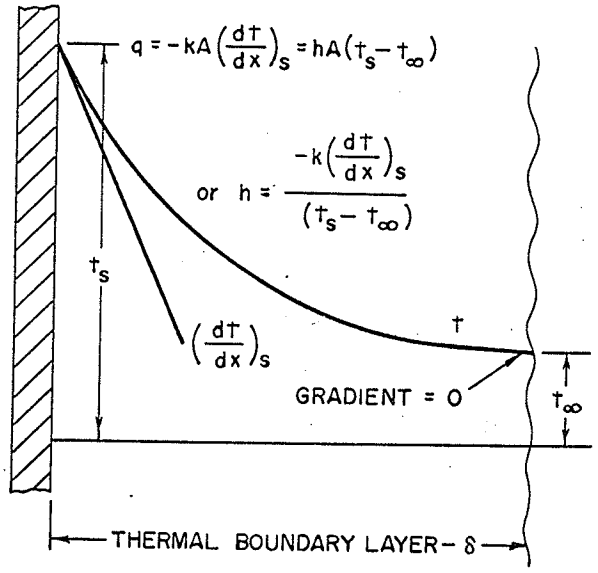

FIGURE 1

PHYSICAL INTERPRETATION OF THE
HEAT TRANSFER COEFFICIENT

From the above considerations, another definition of convection can be formulated which describes convection[3] as "a combination of mechanical and thermal flow, namely, the transportation of heat energy by relatively large masses of the fluid in which molecular transportation (heat conduction) is included".

HYDRODYNAMIC BOUNDARY LAYER EQUATION FOR LAMINAR FLOW

A hydrodynamic or velocity boundary layer may be described as a region around a body where a velocity field is

disturbed. To illustrate the boundary layer, consider an unbounded incompressible viscous fluid flowing with uniform velocity over a thin flat plate. As the fluid passes over the leading edge of the plate, the friction between the surface and the layer of fluid adjacent to it theoretically brings the layer to rest. Viscous forces between this layer and adjacent layers of fluid reduce their velocities in successive stages. A plot of the velocities of these layers yields the shape of curve shown in Figure 2. The portions of the fluid in which the friction and viscous forces are controlling the velocity, are known as the hydrodynamic boundary layer.

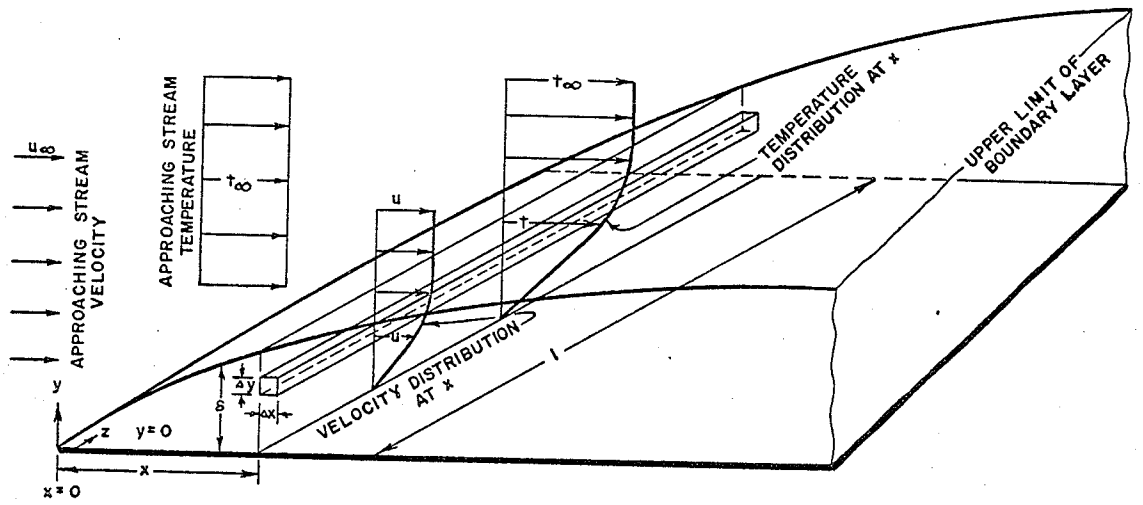

FIGURE 2

THE VELOCITY AND TEMPERATURE DISTRIBUTIONS IN A LAMINAR BOUNDARY LAYER ALONG A FLAT PLATE

To determine the differential equations which apply to this system, consider a unit width of the plate outlined in Figure 2, taken somewhere near its centre, to eliminate any side effects. A momentum, energy and mass balance for the small parallelepiped-shaped volume (ΔX x ΔY x 1) shown in Figure 3 enables a theoretical analysis.

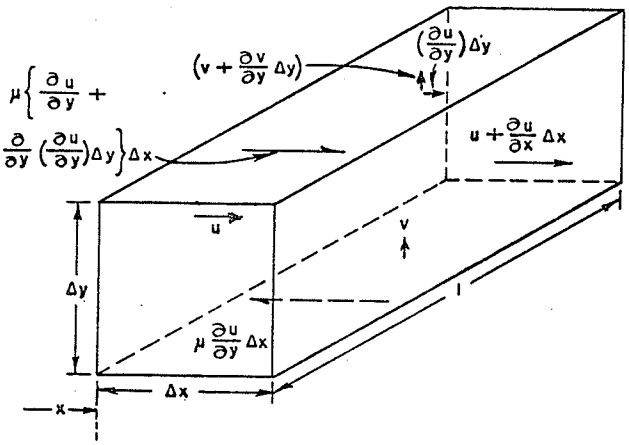

FIGURE 3

VELOCITY CHANGES AND VISCOUS FORCES ACTING ON ELEMENTAL VOLUME FROM FIGURE 2

Since viscous and inertia forces are the most significant in the boundary layer, the pressure forces can be neglected as they are of second order of magnitude. Pertinent quantities are shown in two dimensions in Figure 3. Equating the momentum change per unit time to the forces acting in the X-direction yields

$$u\frac{\partial u}{\partial x} + v\frac{\partial u}{\partial y} = \nu\frac{\partial^2 u}{\partial y^2} \quad \ldots\ldots\ldots\ldots\ldots\ldots\ldots\ldots\ldots\ldots (7)$$

which is a two dimensional equation of motion for the hydrodynamic boundary layer for laminar flow.

THERMAL BOUNDARY LAYER EQUATION FOR LAMINAR FLOW

The thermal boundary layer may be described as a region around a body where a temperature field builds up if the body is being heated or cooled. The diagram in Figure 2 illustrates the thermal boundary layer in comparison to the hydrodynamic boundary layer previously referred to. If the two layers are of the same thickness, the temperature and velocity distributions may be similar, each increasing from zero at the plate to free stream conditions at the upper limit of the boundary layer.

An equation for the thermal boundary layer can be developed with the aid of Figure 4, which shows the energy quantities entering and leaving the elemental volume of Figure 2. As the rate of temperature change in the X-direction is small, it is neglected as a first approximation. Since the temperature in the system varies only with location and not with time, all energy quantities entering the volume must equal zero.

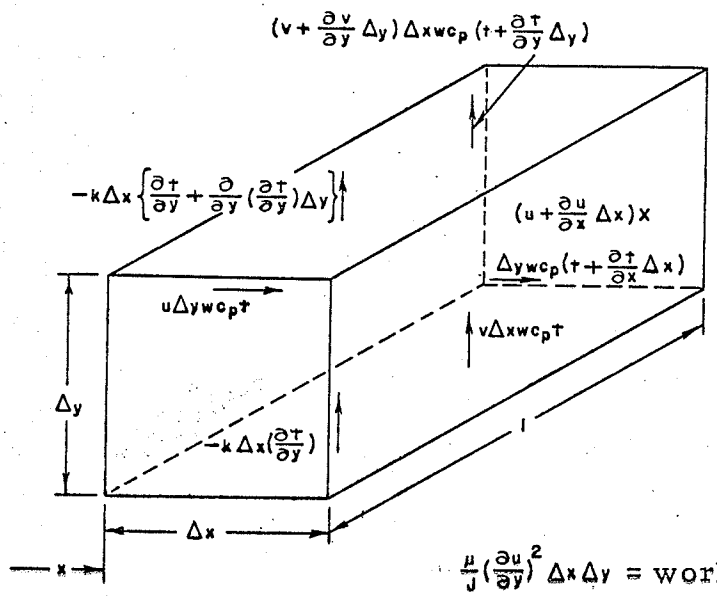

$\frac{\mu}{J}(\frac{\partial u}{\partial y})^2 \Delta x \Delta y$ = work done by element in overcoming viscous drag

FIGURE 4

ENERGY QUANTITIES ENTERING AND LEAVING ELEMENTAL VOLUME IN FIGURE 2

Combining above with the fact that a mass balance across the element equals zero, leads to the thermal boundary layer equation:

$$u\ \frac{\partial t}{\partial x} + v\ \frac{\partial t}{\partial y} = \frac{K}{WCp}\ \frac{\partial^2 t}{\partial y^2} + \frac{\mu}{JWCp}\left(\frac{\partial u}{\partial y}\right)^2 \quad (8)$$

In order to evaluate the temperature field in the boundary layer, a case similar to the above is considered with relatively low free stream velocity and with a small temperature diff-

erence between plate and free stream. For the above conditions the effect of frictional heat generated, expressed by the term $\mu (\partial u/\partial y)^2 / WC_pJ$ can be neglected and Equation (8) simplifies to:

$$\frac{u\,\partial t}{\partial x} + \frac{v\,\partial t}{\partial y} = \frac{\alpha \partial^2 t}{\partial y^2} \quad \ldots\ldots\ldots\ldots\ldots\ldots (9)$$

where K/WC_p is replaced by the thermal diffusivity, α. For $\alpha = \nu$ Equation (9) is identical to Equation (7) with "t" replacing "u", it follows then, that for such a case, the temperature and velocity distribution would be identical. This result has practical significance since for gases "α" is approximately equal to "ν"; it follows that the difference between temperature and velocity profiles will increase as the ratio ν/α differs from unity. The ratio ν/α recognized as $\mu/K/C_p$ is an important dimensionless parameter containing the relative thermal properties of a fluid and is known as the Prandtl Number or modulus:

$$N_{Pr} = \nu/\alpha = \mu C_p/K \quad \ldots\ldots\ldots\ldots\ldots\ldots (10)$$

SOLUTION OF BOUNDARY LAYER EQUATION FOR LAMINAR FLOW IN TUBES

When a liquid or gas flows through a tube, the tube wall is heated or cooled causing a thermal boundary layer to build up along the tube walls. The boundary layers become thicker up to a certain point where they meet on the axis at a certain distance from the starting cross section. The length of tube over which the thermal boundary layer is building up is known as the entrance region; after this distance along the tube, the flow is said to be fully developed for which the velocity profile has the shape of a parabola. This flow condition is usually referred to as Poiseuille flow.[4]

The heat transfer to the walls of a tube under conditions of Poiseuille flow has been calculated by Grätz, Callendar and Nusselt by a solution of differential equations. The energy equation was derived from an energy balance on a ring-shaped volume element of length " dx", radius " r " and width "dr" located in the flow concentrically with respect to the tube axis. An account of the heat transported by conduction and convection in the radial direction for the case of constant heat flow at the wall, results in the following expression for the temperature profile:

$$\theta = t - t_w = \frac{2 \rho C_p u_m R^2}{K} \frac{\partial t}{\partial x}$$

$$\left[\frac{1}{4} \left(\frac{r}{R} \right)^2 - \frac{1}{16} \left(\frac{r}{R} \right)^4 - \frac{3}{16} \right] \quad \ldots\ldots\ldots\ldots\ldots\ldots \quad (11)$$

For fully developed flow, the temperature profile is the same at any station "x" and the heat transfer coefficient is determined by the temperature gradient at the wall. From the above equation, exact solutions are obtained for the Nusselt Number based on the local difference between wall temperature and fluid bulk temperature:

$$N_{Nu_d} = 4.36 \text{ for a constant heat rate} \quad \ldots\ldots\ldots \quad (12)$$

and

$$N_{Nu_d} = 3.65 \text{ for a constant wall temperature} \quad \ldots\ldots \quad (13)$$

Eckert has developed an approximate solution for fully developed laminar flow conditions, this solution is expressed as:

$$N_{Nu_d} = 4.12 \quad \ldots\ldots\ldots\ldots\ldots\ldots\ldots\ldots\ldots\ldots \quad (14)$$

Equation (14) gives results 6 per cent smaller than Equation (12), and 13 per cent larger than Equation (13).

The above solutions are developed for constant property conditions, and consequently differ somewhat from test results of various observers, as most tests in the laminar flow range are carried out using high viscosity liquids. As the viscosity varies with temperature, the velocity profile is changed, thus affecting the temperature profile and the heat transfer characteristics.

LAMINAR AND TURBULENT FLOW IN TUBES

Osborne Reynolds proved in 1883 that there are basically two different forms of flow, namely, laminar and turbulent. In laminar flow the individual streamlines run in an orderly manner side by side, while in turbulent flow the streamlines are interwoven with each other in an irregular manner.

In going from laminar to turbulent flow conditions, the medium goes through a transition zone, in which the particles of the flowing fluid start oscillating and eventually become irregular in shape and transform into vortices which are characteristic of turbulent flow.

As air flows over a flat plate as shown in Figure 5, a boundary layer forms at the leading edge. Its thickness increases towards the rear and at a certain distance Lc from the leading edge, the flow within the boundary layer which at first is laminar changes to turbulent. Within the turbulent boundary layer there still exists a thin laminar film of thickness "δ_b" next to the surface as shown in Figure 5. This film thickness was found to vary from $0.02\delta_{tu}$ to $0.00005\,\delta_{tu}$, where δ_{tu} is the thickness of the fully developed turbulent boundary layer.

The distance Lc decreases as the velocity " u_∞" is increased such that the product u_∞ Lc remains unchanged. Reynolds discovered that the change from laminar to turbulent flow takes place at a critical value of the dimensionless term u_∞ Lc/ν which is referred to as the Reynolds Number or modulus. Factors such as roughness, shape of leading edge of plate and presence of a turbulence grid in the fluid stream all tend to lower the value of the critical Reynolds Number.

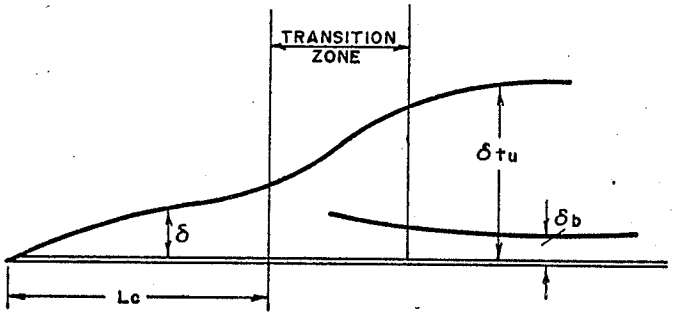

FIGURE 5

LAMINAR AND TURBULENT LAYERS
ON A FLAT PLATE

The flow conditions in a pipe at the vicinity of the inlet are similar to the conditions for flow over a plate in parallel flow. As shown in Figure 6, the boundary layer increases from zero thickness at the inlet, to a maximum value at some distance Lc down the pipe at which point the boundary layers become so thick

that they make contact with each other.

Depending on whether the boundary layers are laminar or turbulent, the velocity profile after this length "Lc" will approach the form of either a parabola or an arched curve as shown in Figure 6. The velocity profile further downstream from this point does not change, thus, the flow is then referred to as fully developed. As in the case of the flat plate the flow becomes turbulent if the Reynolds Number (N_{Re_c}) exceeds a certain critical value. For flow in smooth tubes, this critical value is usually taken at about 2300, but depending on conditions such as roughness and degree of agitation, this value may change considerably.

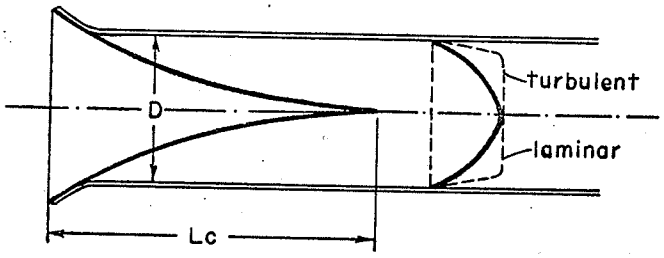

FIGURE 6

FLOW IN A TUBE NEAR INLET

Various methods have been used to determine the critical value of N_{Re_c}, all of which agree quite closely, as shown in Table I.

TABLE I

CRITICAL REYNOLDS NUMBER N_{Re_c} FOR SMOOTH CIRCULAR PIPES DETERMINED BY DIFFERENT METHODS OF OBSERVATION[5]

METHOD	CRITICAL VALUE OF N_{Re_c}
Pipe friction	Between 2,100 and 2,300
Color Band	Above 2,000
Stethoscope	Between 1,890 and 2,130
Motion of Coloidal particle	Between 2,000 and 3,700

THEORETICAL METHODS APPLIED TO TURBULENT FLOW REGION IN TUBES

Investigation of the velocity distribution in pipes during turbulent flow conditions indicate the presence of three distinct zones, a laminar sublayer, a buffer layer, and a turbulent core. Due to different characteristics of each region, the heat resistance by each layer must be calculated separately. Equating the heat flows through the various boundary layers, and using shear stress and velocity ratio relations, enables the development of Equation (15)

$$N_{St} = \frac{h}{\rho C_p u_m} = \frac{0.0384 (N_{Re_d})^{-1/4}}{1 + A (N_{Re_d})^{-1/8} (N_{Pr}-1)} \quad \ldots(15)$$

where A is given by Hoffman as $A = 1.5 N_{Pr}^{-1/6}$.

The left hand side of Equation (15) consists of a dimensionless parameter known as the Stanton Number which is often used to correlate experimental data, since it can be evaluated without determination of physical properties.

Equation (15) was developed for constant property values. Hoffman investigated the influence of the variability of the property values on heat transfer, and found that Equation (15) holds true when the property values are inserted at a reference temperature t^* where:

$$t^* = t_B - \frac{0.1 N_{Pr} + 40}{N_{Pr} + 72} (t_B - t_w) \quad \ldots\ldots\ldots(16)$$

The reference temperature is a function of N_{Pr} only, and consequently must be considered as a first approximation, as it must be expected that the heat transfer in fluids with variable properties will depend on how the properties vary with temperature and pressure.

Another solution may be developed by considering the fluid flow in the pipe as laminar at the wall, and being subject to an irregular eddying type motion within the centre of the tube. It is useful to define an eddy viscosity or eddy diffusivity for momentum ϵ_m by:

$$\tau_t = \rho \epsilon_m \frac{du}{dy} \quad \text{.....(17)}$$

Similarly, an expression for turbulent diffusivity of heat may be defined as:

$$Q_t = -\rho Cp \epsilon_q \frac{\partial t}{\partial y} \quad \text{.....(18)}$$

From expressions for ϵ_m in the laminar sublayer, the buffer layer and the turbulent core, and the definition $\epsilon_q = E \epsilon_m$ the following expression for the temperature drop between pipe surface and centre was developed by Giedt [2]:

$$t_s - t_c = \frac{5Q_s}{E\, CpW\, A_s \sqrt{\sigma_s/\rho}} \left[EN_{Pr} + Ln\,(1 + 5EN_{Pr}) + 0.5\, Ln \frac{N_{Re}}{60} \sqrt{\frac{f}{8}} \right] \quad (19)$$

The three terms in the brackets of Equation (19) can be considered as indicating the proportionate resistance of the three fluid layers. Equations for the dimensionless temperature distribution in any layer may be obtained by taking the ratio of the thermal resistance from the wall to any point "y", to the total resistance. For the laminar sublayer this becomes:

$$\frac{t_s - t}{t_s - t_c} = \frac{EN_{Pr}\, y/y_1}{EN_{Pr} + Ln\,(1 + 5E\, N_{Pr}) + 0.5\, Ln \frac{N_{Re}}{60} \sqrt{\frac{f}{8}}} \quad (20)$$

Differentiation of Equation (20) and accounting for the influence of molecular conduction in the turbulent core by including the factor "F", yields the following relation for the Stanton Number:

$$N_{St} = \frac{E \sqrt{f/8} \left(\frac{t_s - t_c}{t_s - t_b}\right)}{5 \left[EN_{Pr} + Ln\ (1 + 5EN_{Pr}) + 0.5\ F\ Ln\ \frac{N_{Re}}{60}\sqrt{\frac{f}{8}} \right]} \quad (21)$$

LOCAL AND AVERAGE HEAT TRANSFER COEFFICIENTS

The heat transfer coefficient was defined in a previous section as a measure of the convective capacity of the flowing fluid, and was defined for the flat plate system by Equation (6)

$$h = \frac{-K}{ts - t_\infty} \left(\frac{dt}{dx}\right)_s \quad \ldots\ldots\ldots\ldots\ldots\ldots\ldots\ldots\ldots\ldots (6)$$

where: $(dt/dx)s$ = the slope of the temperature gradient at the surface

$t_s - t_\infty$ = temperature difference between the plate surface and surrounding media.

The above relation can be used to define two heat transfer coefficients, one, a local coefficient denoted by h_x and the other, an average coefficient denoted by h_a. For flow in tubes the local coefficient h_x is a measure of the heat

transfer rate at a specific distance "x" from the tube inlet, while the average coefficient h_a represents an average heat transfer rate over the tube length "L".

The local heat transfer coefficient may be defined in terms of the difference between the wall temperature t_s and the mean fluid temperature t_m at that point, i.e.:

$$\frac{Q(x)}{A} = h_x (t_s - t_m) = -K \left(\frac{\partial t}{\partial r}\right)_{r_1, x} \quad \ldots\ldots\ldots\ldots\ldots\ldots (22)$$

where $t_m = \frac{1}{Um\ \pi r_1^2} \int_o^{r_1} ut\ 2\pi r\ dr$ ..... (23)

The average heat transfer coefficient h_a over a length "L" can be defined by the relation:

$$Q = h_a\ A\ (t_s - t_m) \quad BTU/hr \quad \ldots\ldots\ldots\ldots\ldots\ldots (24)$$

where: t_s and t_m are average surface temperature and average fluid temperature respectively over a length "L". The average heat transfer coefficient can also be defined as the average of the local heat transfer coefficient over the length "L" i.e.:

$$h_a = \frac{1}{L} \int_o^L h_x\ d_x \quad \ldots\ldots\ldots\ldots\ldots\ldots\ldots\ldots (25)$$

As the temperature distribution varies along the pipe length, it follows that the local "h_x", which varies as the slope of the temperature gradient at the wall, will vary along the tube length until the temperature distribution has become fully established, and will then remain constant. The average "h_a" will likewise vary along the tube length from a high value near the tube inlet, then decrease along the tube length to an almost constant value after the flow has become fully developed.

From the definition of the heat transfer coefficient, as the slope of the temperature distribution at the surface, it is possible to define a dimensionless heat transfer coefficient by the relation hD/K, where

h = the local heat transfer coefficient "h_x" or the average heat transfer coefficient "h_a"

D = the inside diameter of the tube - ft.

K = the thermal conductivity of the fluid.

The term $\frac{hD}{K}$ represents the dimensionless slope of the temperature distribution at the surface, and is usually referred to as the dimensionless heat transfer coefficient, and known as the Nusselt Number or Modulus.

Depending on whether the local or the average heat transfer coefficient is used; the corresponding term will yield the local or average Nusselt Number respectively.

SEMI-EMPIRICAL ANALYSES AND DESIGN PRACTICES

DIMENSIONAL ANALYSES

Dimensional Analyses yield a possible form of solution to a process by relating all the physical properties involved, (through their dimensions), and grouping these factors into dimensionless combinations. This system has been used to establish the correlation between various dimensionless factors and the heat transfer coefficient "h" for forced convection conditions. This method gives the following result:

$$h = B\ N_{Re}^{a}\ N_{Pr}^{c}\ K/L \quad \text{.....(26)}$$

where a, B and c are parameters which can readily be evaluated by experiment. Equation (26) may be rewritten in the form:

$$\frac{hL}{K} = B\ N_{Re}^{a}\ N_{Pr}^{c} \quad \text{..... (27)}$$

which is a General Equation for Forced Convection. The term $\frac{hL}{K}$ can be recognized as the Nusselt Number, defined in the previous section, with "L" the characteristic length replacing "D".

Equation (27) can be rewritten as:

$$N_{Nu} = f\ (N_{Re}, N_{Pr}) = f(N_{Pe}) \quad \text{..... (28)}$$

where the product of N_{Re} and N_{Pr} yields a further dimensionless number N_{Pe} known as the Péclet Number which is denoted by

$$N_{Pe} = DGC_p/K \qquad (29)$$

A further combination of dimensionless numbers yields the following relation for the Stanton Number N_{St}:

$$N_{St} = \frac{N_{Nu}}{N_{Re}\,N_{Pr}} = \frac{h}{CpG} \qquad (30)$$

which is a very useful dimensionless number often used for correlating test data.

The Graetz Number, $N_{Gz} = W\ Cp/Kx$ is another useful dimensionless number developed from dimensional analysis.

REYNOLDS ANALOGY

In 1874, Reynolds pointed out that a relationship existed between heat transfer and pressure drop. He later developed an expression for fluids having a Prandtl Number of unity from the knowledge that for this case, the velocity and temperature profiles are identical. Reynolds concluded that for the above noted case, the Stanton Number equals one half the skin friction coefficient, i.e.:

$$N_{St} = C_f/2 \qquad (31)$$

Equation (31) is usually referred to as "Reynolds Analogy".

Further studies on fluids having Prandtl Numbers other than unity have revealed that the relation between the Stanton Number and the skin friction coefficient is approximately expressed by the equation:

$$N_{St}\ N_{Pr}^{2/3} = C_f/2 \quad \text{.....(32)}$$

Equation (32) represents the General Form of Reynolds Analogy.

FORMULAE USED FOR LAMINAR FLOW INSIDE TUBES

This section shall be devoted to the listing of possible methods of solution to a problem involving forced convection for laminar flow inside tubes. The formulae in common usage shall be discussed together with any limitations which apply to them.

The following semi-empirical formula by Hausen[6] representing the average Nusselt Number, is in common usage

$$N_{Nu_m} = \frac{h_m D}{K} = 3.65 + \frac{0.068\,(D/L) N_{Re}\ N_{Pr}}{1 + 0.04\left[(D/L)\ N_{Re}\ N_{Pr}\right]^{2/3}} \quad (33)$$

This formula, applies only for uniform wall temperatures and fully developed flow, and is restricted to constant physical properties of the fluid, i.e., to small temperature differences or

low heat flux.

For large temperature differences, the change in viscosity of the flowing media affects the velocity profile and, therefore, the heat transfer rate. Equation (33) can be applied to larger temperature differences if the right hand side of the equation is multiplied by $(\mu_b/\mu_w)^{0.14}$ where μ_b is the viscosity at the fluid bulk temperature and μ_w the viscosity at the wall temperature.

Sieder and Tate[1] have correlated convection data for laminar flow conditions and have accounted for the influence of temperature on viscosity and, therefore, on flow pattern and heat transfer in the following empirical formula for the average N_{Nu_a}.

$$N_{Nu_a} = 1.86\ (N_{Pe})_a^{1/3}\ (D/L)^{1/3} \left(\frac{\mu a}{\mu s}\right)^{0.14} \quad \ldots\ldots\ldots (34)$$

where "s" and "a" refer to surface temperature and arithmetic mean of the fluid temperature $t_a = \frac{(t_o + t_L)}{2}$ respectively and where t_o and t_L are the entering and leaving temperatures. Equation (34) can also be written as

$$N_{Nu_a} = 1.86\ \sqrt[3]{\frac{4}{\pi}}\ (N_{Gz})^{1/3} \left(\frac{\mu a}{\mu s}\right)^{0.14} \quad \ldots\ldots\ldots\ldots (35)$$

where

$$N_{Gz} = \frac{WC_P}{KL} = \frac{4L}{D\ N_{Re}\ N_{Pr}}$$

is the Graetz Number which is a useful dimensionless number in the study of convection under laminar flow. Equations (34) and (35) are limited to tubes with small diameters where the effects of natural convection are minimized.

It has been found in reviewing published literature that experimental data for the laminar flow of gases are rather scarce. Kays and Nicoll[7] suggest that this may be due to the numerous problems in obtaining accurate results for the low gas flows corresponding to laminar conditions.

As the rate of heat transfer for gases in the laminar flow region is generally low, small unaccountable heat leaks become significant and lead to high inaccuracies in the test results. High temperature differentials are developed at low velocities corresponding to laminar flow, consequently, natural convection can have serious effects on the shape of the velocity profile. Rosen, Hanratty, Scheele et al[8]. claim that for their experiments in the N_{Re} range from 350 to 640, natural convection accounted for 20 - 30% scatter frequency in their results.

METHODS OF DETERMINING THE TRANSITION REGION

The transition region lies between the end of the laminar flow region and the start of a region of well developed turbulent flow. The Reynolds Number N_{Re} corresponding to the lower limit of the transition zone in a tube is normally taken at about 2,300. The upper limit of the transition is generally taken at about N_{Re} of 6,000, but can, depending on conditions, be as high as N_{Re} of 10,000.

Figures 7 (a) and (b) show the different velocity distributions in a pipe, for fluid flow under laminar and turbulent flow conditions respectively. In these illustrations, "V" is the average velocity of the flowing fluid and "V_{max}" is the maximum velocity at the pipe cross-section.

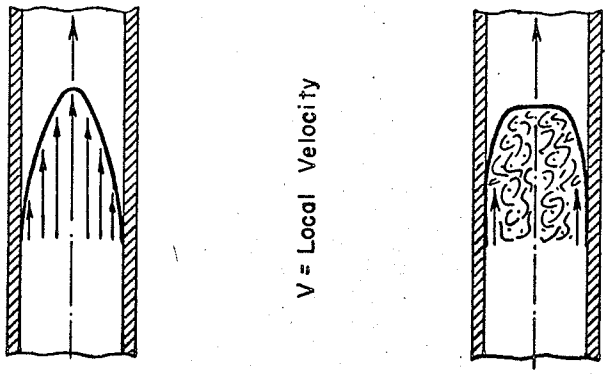

$V/V_{max} = 0.5$ $V/V_{max} = 0.8 \pm$

(a) Laminar Motion (b) Turbulent Motion

FIGURE 7

VELOCITY DISTRIBUTION IN A PIPE

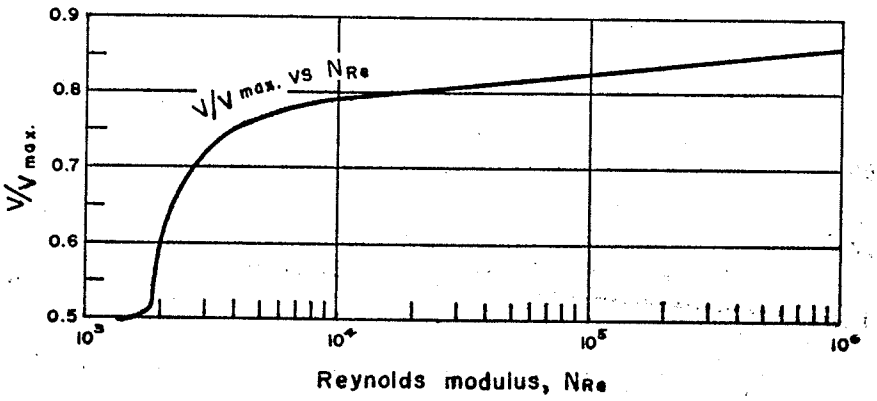

FIGURE 8

RELATION BETWEEN VELOCITY DISTRIBUTION AND REYNOLDS NUMBER

Figure 8 shows that up to N_{Re} of 2,100, V/Vmax is 0.5 while in the range of N_{Re} from 2,100 to 3,000, V/Vmax rises sharply from 0.5 to 0.726 and thereafter increases slowly as Reynolds Number is increased.

The term transition region may also be applied to that section in the tube entrance region where the laminar flow boundary layer on the inner wall has increased in thickness until the boundary layers meet at the centre of the tube. When the boundary layers fill the tube, the flow is said to be fully developed.

It has been found by a number of observers, that the length L_c from the tube inlet at which the flow becomes fully developed, is a function of the Reynolds Number and the type of entry condition. For a bell-mouthed entry, Latzko[5] predicts that for turbulent flow conditions, the length L_c can be determined from the relation:

$$L_c/D = 0.693\ N_{Re}^{1/4} \quad \ldots\ldots\ldots\ldots\ldots\ldots\ldots\ldots\ (36)$$

Under laminar flow conditions, Langharr[2] gives the length L_c by:

$$L_c/D = 0.05\ N_{Re} \quad \ldots\ldots\ldots\ldots\ldots\ldots\ldots\ldots\ (37)$$

It is useful to relate the variation in velocity and temperature profiles in the tube entrance region to the heat transfer rate in this region. Figure 9 illustrates that the local Nusselt Number N_{Nu_x} varies along the tube entrance region up to a certain distance from the tube inlet, after which it remains constant.

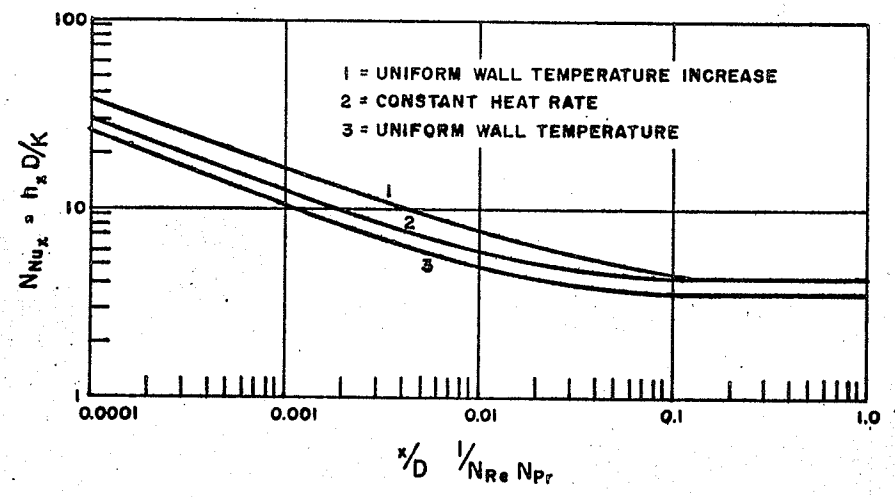

FIGURE 9

VARIATION OF THE LOCAL NUSSELT NUMBER
FOR FULLY DEVELOPED LAMINAR FLOW IN A TUBE

It can be noted from Figure 9 that the constant value of the local Nusselt Number N_{Nu_x} is 3.65 for a uniform wall temperature. For a constant heat rate, or a uniform increase in wall temperature Giedt[2] gives 4.36 as the constant value for the local Nusselt Number. According to Figure 9, the local Nusselt Number N_{Nu_x} becomes constant when

$$\frac{X}{D} \times \frac{1}{N_{Re}\ N_{Pr}} = 0.05$$

Thus, the length L_c in which the temperature distribution is changing can be estimated by:

$$\frac{L_c}{D} = 0.05\ N_{Re}\ \ N_{Pr} \quad \ldots\ldots\ldots\ldots\ldots\ldots\ldots\ldots (38)$$

A comparison of Equations (37) and (38) shows that they differ only by N_{Pr}. Thus, for fluids with small N_{Pr}, the thermal transition length is short as compared to the velocity transition length, while the converse is true for fluids having large N_{Pr}. For N_{Pr} of unity the velocity and thermal transition lengths are identical as previously suggested. From the behaviour of the local N_{Nu_x} along the tube entrance length, and the relation between h_x and N_{Nu_x} it follows that the local h_x will also reach a constant value at the length L_c.

Equation (36) gave the distance L_c for a bell-mouthed entry and turbulent flow conditions as: $L_c = D \times 0.693\ N_{Re}^{1/4}$. For lengths other than the critical length predicted in Equation (36) the mean heat

transfer coefficient h_m (from L of 0 to L) may be calculated for turbulent flow conditions from the following relations, where h_∞ is the local heat transfer coefficient at the critical length L_c.

$$\frac{h_m}{h_\infty} = 1.11 \left[\frac{(DG/\mu)^{1/5}}{(L/D)^{4/5}}\right]^{0.275} \quad \text{.....(39)}$$

$$\frac{h_m}{h_\infty} = 1 + \frac{CD}{L} \quad \text{.....(40)}$$

$$\frac{h_m}{h_\infty} = 1 + (D/L)^{0.7} \quad \text{.....(41)}$$

Equation (39) was developed by Latzko[5] and applies to lengths less than the critical length L_c. Recent data by Boelter, Young and Iverson has substantiated this equation.

Equation (40) was also developed by Latzko and applies to lengths greater than the critical length L_c. The value of C in Equation (40) is represented by:

$$C = 0.144\ (DG/\mu)^{1/4} \quad \text{.....(42)}$$

From recent data for a bell-mouthed entry, for N_{Re} from 26,000 to 56,000 Boelter, Young and Iverson[5] found a value of C=1.4.

Equation (41) is recommended by Kroll[5] for sharp edged entrances and for gases under turbulent flow for L/D up to 60. For L/D greater than 60, Kroll claims that the ratio h_m/h_∞ approaches unity.

Equation (43) was developed for air in tubes by Ermolin[9], he states that for L/D values less than or equal to 40:

$$N_{Nu_x} = 0.0145\ N_{Re}^{0.83}\ N_{Pr}^{0.4}\ (1 + K_x\ D/x) \quad \ldots\ldots (43)$$

where K_x, for x/D greater than or equal to 5, is dependent on N_{Re}, and for x/D less than 5, the local N_{Nu_x} drops rapidly to x/D = 5.

The effect of L/D on the heat transfer coefficient for gases was illustrated in the preceding paragraphs. Figure 10 illustrates the correlation made for liquids by Sieder and Tate[1] and indicates that the effect of L/D is also important for liquids, particularly in the laminar and transition regions.

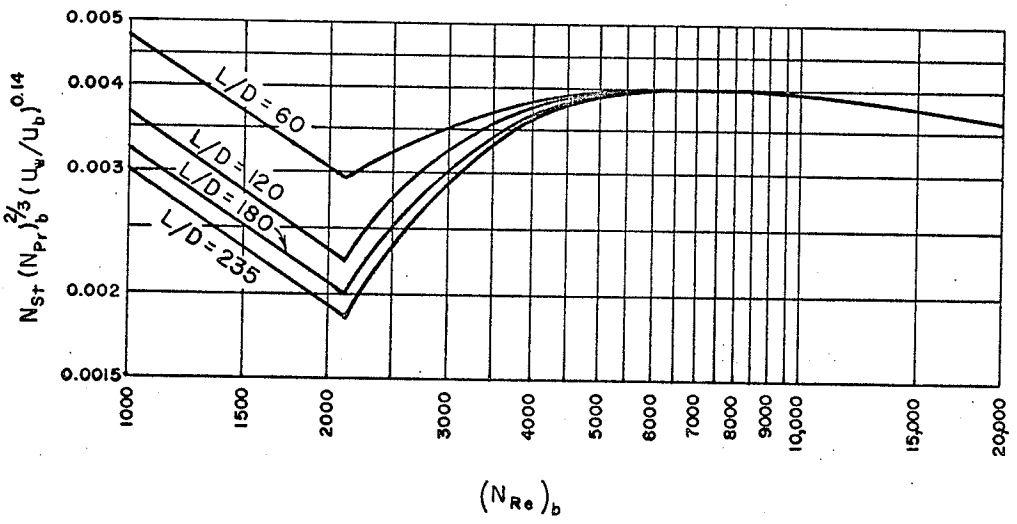

FIGURE 10

DIMENSIONLESS REPRESENTATION OF HEAT TRANSFER IN SEMI TURBULENT FLOW

FORMULAE USED FOR TURBULENT FLOW INSIDE TUBES

This section deals with the various formulae available for solving problems of forced convection involving flow inside tubes.

The formulae in common usage are discussed, together with any limitations which apply to them.

Evaluation of the parameters in Equation (27) has been done by a number of observers over a moderate temperature range, for conditions ranging from Prandtl Numbers of 0.7 to 120, for Reynolds Numbers from 10,000 to 120,000, and for L/D of 60 or more. The results of various observers are represented in the following semi-empirical equations:

$$N_{Nu} = 0.0243 \ (N_{Re})^{0.8} \ (N_{Pr})^{0.4} \quad \text{.....(44)}$$

$$N_{Nu} = 0.0265 \ (N_{Re})^{0.8} \ (N_{Pr})^{0.3} \quad \text{.....(45)}$$

$$N_{Nu} = 0.027 \ (N_{Re})^{0.8} \ (N_{Pr})^{1/3} \ (\mu_b/\mu_w)^{0.14} \quad \text{(46)}$$

$$N_{Nu} = 0.036 \ (N_{Re})^{0.8} \ (N_{Pr})^{1/3} \ (\mu_b/\mu_w)^{0.14} \ (D/L)^{1/18} \quad \text{.....(47)}$$

$$\frac{h}{C_{pb}G} = \left(\frac{C_p\mu}{K}\right)_f = \frac{0.023}{(DG/\mu_f)^{0.2}} \quad \text{.....(48)}$$

It can be noted from the above equations that most observers agree with the form of the equation, but give slightly different constant factors and exponents for N_{Pr} to account for heating and cooling. Equations (44) and (45) were developed from the results of Dittus and Boelter and apply for heating and cooling, respectively, of the fluid inside the pipe.

Equation (46) developed by Sieder and Tate is made

applicable to heating and cooling by applying the ratio $(\mu_b/\mu_w)^{0.14}$ to account for the varying viscosity. All properties except μ_w in Equation (46) are evaluated at the bulk temperature. Equation (47) was developed by Burbach, Eagle and Ferguson from the results of their tests in the range of L/D from 10 to 400. This equation accounts for the variation in the heat transfer coefficient with tube length by including the factor $(D/L)^{1/18}$. All properties in Equation (47) except μ_w are evaluated at the bulk temperature. Cholette[1] recommends that the influence of the tube length to diameter ratio D/L is best expressed by $(D/L)^{1/10}$ in lieu of $(D/L)^{1/18}$ as proposed in Equation (47).

Equation (48) suggested by Colburn[5] has all the properties except Cp in the Stanton Modulus evaluated at the "film" temperature. The "film" temperature is usually taken as the arithmetic average of the wall and bulk temperature. Colburn claims that the form of Equation (48) has several advantages in correlating data. He defines a heat transfer factor "J" such that:

$$J = \frac{h}{\rho u Cp} \left(\frac{\mu Cp}{K}\right)^{2/3} = N_{St} N_{Pr}^{2/3} \quad \text{.....(49)}$$

where $h/\rho u Cp$ is recognized as the Stanton Number. For laminar and turbulent flow in smooth tubes, Colburn found that the factor "J" was equal to one half the skin friction coefficient, thus,

$$J = C_f/2 = \frac{0.023}{(DG/\mu_f)^{0.2}} = N_{St} N_{Pr}^{2/3} \quad \text{.....(50)}$$

which confirms the General Form of Reynolds Analogy stated in Equation (32).

DESIGN CONSIDERATIONS

As the local heat transfer coefficient is largest at the tube entrance and decreases in the direction of flow up to a certain critical distance, the tubes should be kept as short as possible to be most effective from a heat transfer point of view. As there is considerable pressure drop in tube entrances, the high pressure drops encountered with numerous short tubes would offset the heat transfer advantages.

There are practical limitations to the size and shape of heat exchangers. It is, therefore, the designer's duty, to select the proper number of tubes and the best length to diameter ratio, to make up a heat exchanger having a practical size and high efficiency.

Theoretical considerations and data from various observers point to the fact that turbulence increases the heat transfer rate. The designer then has the choice of selecting the size and number of tubes which will yield the highest tube velocity and consequently, the most turbulence. When it is not possible to cause turbulence by increasing the flow velocity, it is sometimes

practical to induce turbulence by using mixing devices or turbulators, which have the effect of artificially roughening the pipe surface.

Data from various observers confirm the advantages of a rough surface from a heat transfer standpoint. Lancet[10] states:

$$N_{Nu_m} = 0.042 \quad N_{Re}^{0.8} \quad N_{Pr}^{1/3} \text{ for a rough duct....(51)}$$

as compared to Colburn's

$$N_{Nu_m} = 0.023 \quad N_{Re}^{0.8} \quad N_{Pr}^{1/3} \text{ for a smooth pipe..(52)}$$

A similar improvement in heat transfer rate was substantiated by Dipprey and Sabersky[11]. It was established, however, by a number of observers[10 12 13], that the effect of roughness has a larger effect on the friction factor C_f (pressure drop) than it does on the heat transfer factor C_H. It follows then, that if pressure drop is taken into consideration, a smooth tube is a more efficient heat transfer surface than a rough one.

If the friction losses are taken into consideration in the design of heat exchangers, it follows that the designer must sacrifice heat transfer advantages to reduce the pressure drop.

PART TWO

EXPERIMENTAL STUDIES

PURPOSE OF TEST AND CRITERION OF EQUIPMENT DESIGN

The purpose of the test was to establish the local and average heat transfer coefficients in a pipe for conditions of flow ranging from laminar to turbulent.

Test equipment was set up consisting of two concentric pipes arranged as shown in Figures 11 to 13. The equipment was set up to pass air longitudinally through the inner pipe, and water in cross-flow through the annulus. Air and water were selected as test media, partly due to their availability but mainly due to the relative ease in taking measurements with these media. Air was considered for both media; however, the heat transfer characteristics of air are rather poor as compared to water, consequently, small temperature differences would have been obtained resulting in higher relative inaccuracies. Furthermore, inaccurate estimates of the convective heat transfer coefficient in the annulus would have affected the results considerably more than for water. As air flow through the annulus would have been very difficult to measure, thecombination of air in the inner pipe and water in the annulus was selected.

To maintain a uniform wall temperature over the entire

length of the test section, the annulus was cooled by passing water in cross-flow over the inner pipe. The annulus was divided in a number of sections to enable the observation of heat gains by the water (heat loss by the air) along the incremental lengths of the test section. The sections were kept small to maintain a uniform temperature of the cooling fluid within each section by eliminating the possibility of short circuiting within the section. The small temperature difference within any one section and between adjacent sections reduced the possibility of longitudinal heat transfer from one section to another, thus maintaining a constant axial temperature gradient.

To reduce the heat gains from the jacketed end sections, the ends of the first and last sections of the annulus were insulated with one inch of insulation. However, this insulation proved rather inadequate, as it was evident from the test results that considerable heat was gained by the water in the end sections.

One feature which was incorporated in the design of the test equipment, (although not used for the test) was the installation of test connections in the inner pipe with corresponding conduits through the annulus to the outer pipe to enable taking temperature readings at various points along the tube length. This feature may be used to good advantage should anyone wish to use this test rig for future research on this subject.

General Views of Test Equipment

FIGURE 11

PHOTOGRAPHS OF TEST EQUIPMENT

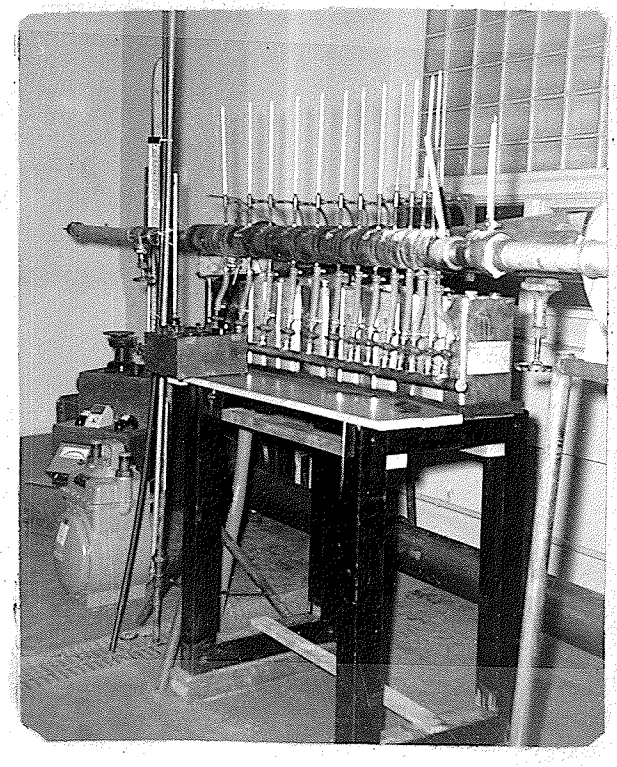

Close-up of Equipment Showing Water Piping and Thermometers

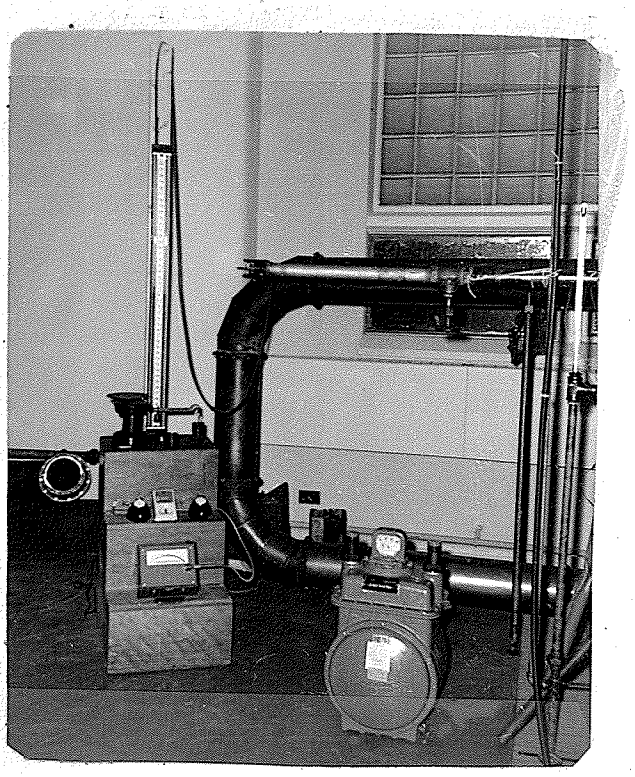

Close-up of Air Measuring Equipment

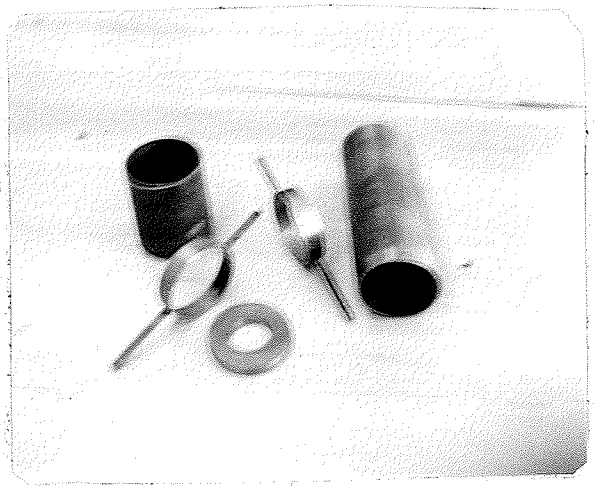

Sections of the Outer Pipe Before Assembly

FIGURE 12

PHOTOGRAPHS OF TEST EQUIPMENT

DESCRIPTION OF EQUIPMENT

A Sir Godfrey and Partners heat pump unit consisting of a diesel driven centrifugal compressor and turbine assembly was used to supply air for testing purposes. The heat pump unit which is normally used as a heating and air conditioning unit operates as outlined below. Air is compressed in a diesel driven centrifugal compressor and passed through a turbine where it expands to discharge conditions and delivered to the space. The unit discharge air temperature can be controlled by varying the compressor speed, by various degrees of re-heating or intercooling between compressor and turbine, or by varying the air flow through the turbine portion of the unit. In passing through the turbine the air does work, and consequently, helps to drive the air compressor by means of the connecting drive assembly.

As it was desirable for test purposes to maintain an air supply as hot as possible, the turbine portion of the heat pump unit was by-passed for all tests. The temperature of the air entering the test section could be varied by changing the speed of the compressor, thus varying the compression ratio, and consequently, the discharge temperature. For most tests the inlet air temperature was kept as high as possible in order to maintain an appreciable temperature difference between air and water and, consequently, a

higher heat flux.

To reduce fluctuations in the supply air pressure to the test equipment, air from the compressor was discharged directly into a receiver tank, and from there it was piped to the test section. A long length of pipe was placed ahead of the test section to reduce the turbulence caused by a sudden contraction at the tank and to attain fully developed flow.

In order to eliminate the disturbing effect of the valve placed downstream to control the amount of air flow through the test section, a length of pipe having an inner diameter equal to the test section was welded between the test section and the valve. Downstream of the control valve, an additional length of straight pipe was installed in order to obtain fully developed flow at the impact tube traverse. The impact tube was used in conjunction with a precision manometer to measure air flows at high flow conditions. At low flow conditions air flow measurements were carried out using a positive displacement meter connected downstream of the flow control valve.

The connecting pipe between the surge tank and the test section was jacketed by means of a concentric pipe arrangement as shown in Figures 13 and 14. Air from the tank was supplied to this jacketed section through a by-pass. This piping arrangement made it possible to obtain the air temperature entering the test section

without placing a thermometer in the air stream which would have disturbed the flow. The total air supplied by the compressor was the sum of the air flowing through the test section and through the by-pass.

The discharge air temperature was measured with a thermocouple placed a short distance beyond the end of the test section, to avoid disturbing the flow within the test section. The length of inner pipe between the end of the test section and the temperature measuring point was jacketed similar to the inlet section, except that no air was by-passed to it.

The cooling water to the various sections was supplied through a common header, thus maintaining a uniform supply water temperature to all sections. To eliminate the effect of pressure fluctuations in the system water supply, a standpipe was set up as shown in Figure 13. This arrangement maintained a constant head of water at all times to the supply header. The individual connections from the water supply header to each annulus section were equipped with control valves enabling the control of water flow through each section, to maintain an equal discharge temperature from all of them. Buckets were used to collect the water passing through each section. Thermometers were used on the supply header and on individual discharges from each section.

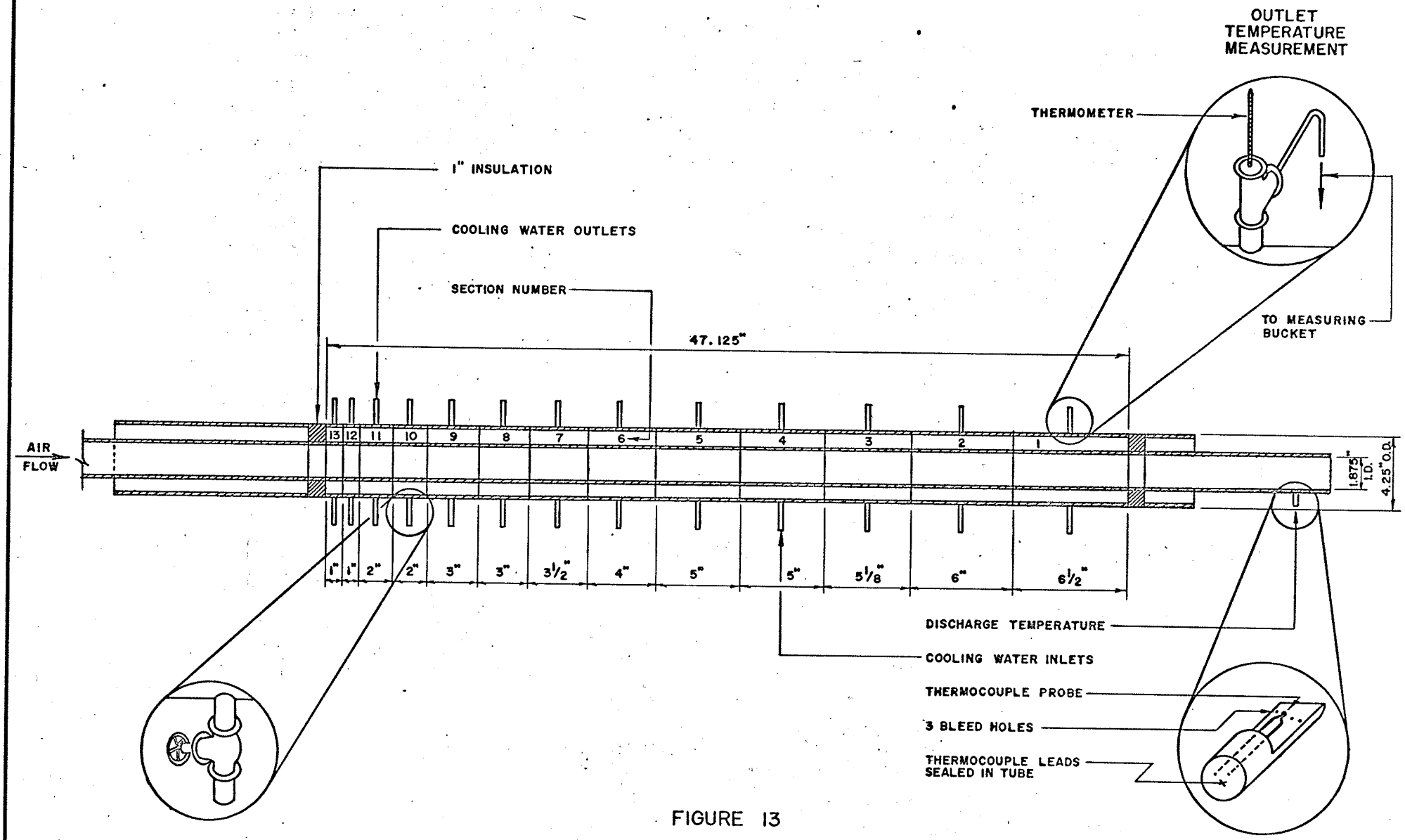

FIGURE 13

DETAIL OF TEST SECTION

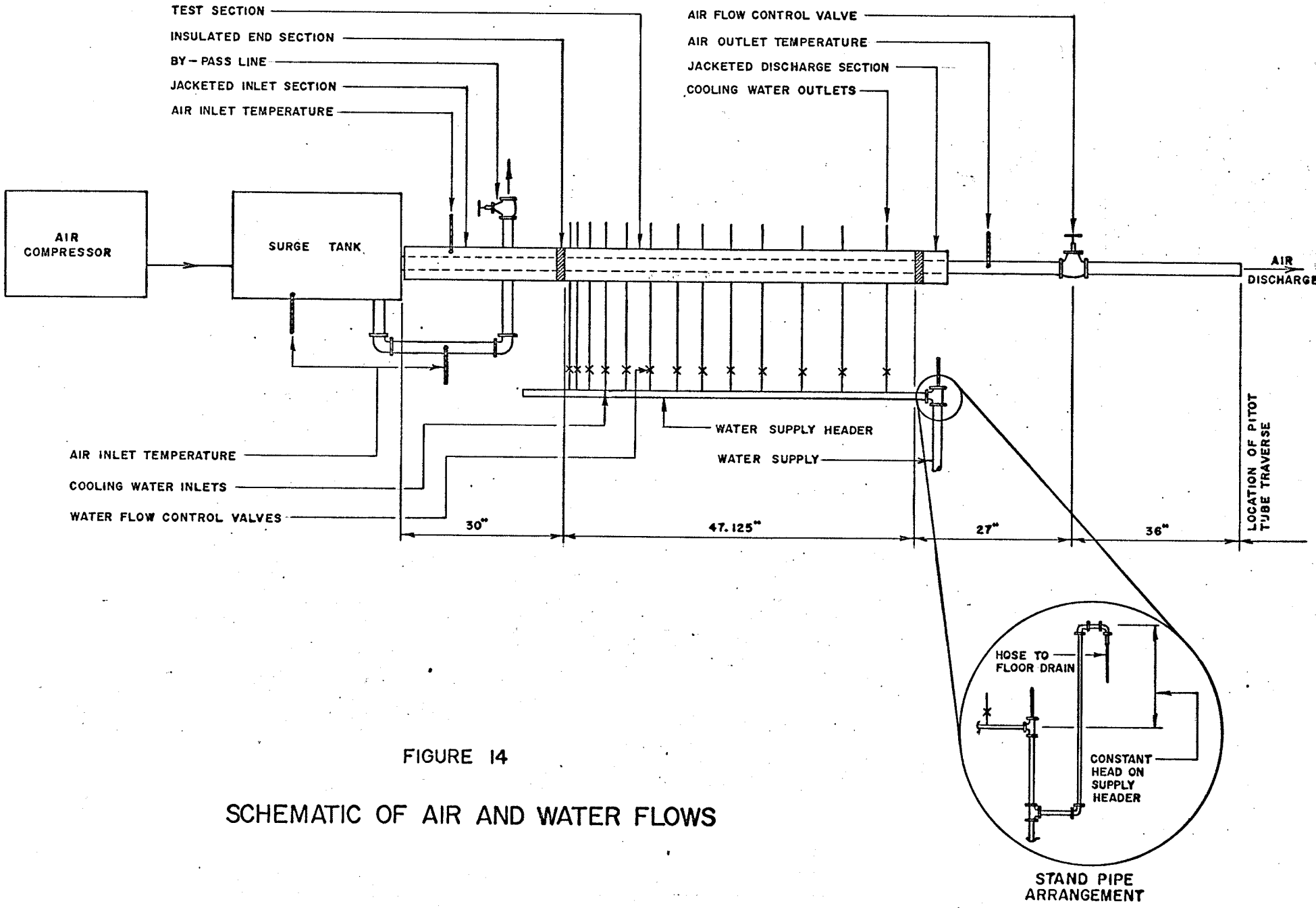

FIGURE 14

SCHEMATIC OF AIR AND WATER FLOWS

TESTING PROCEDURE

The diesel driven compressor was allowed to run at least one half-hour before each test in order to have the system supply air temperature reach equilibrium before each test.

The volume of air passing through the test section was adjusted for each test by opening or closing the valve on the discharge end of the test equipment. The remainder of the air from the compressor was discharged through the by-pass. Once equilibria in air flows was achieved, the water flows to the various sections of the annulus were adjusted to maintain a uniform discharge temperature from each section. This was very difficult to achieve, as a very minute change in valve opening caused an appreciable change in water flow, and therefore, of discharge temperature. The water inlet temperature to all sections was equal as these were all supplied from a common header. Once the valves were adjusted to maintain equal discharge temperatures, the test was started and run for twenty or thirty minutes. The first fifteen tests were run for thirty minutes and the remainder for twenty minutes. The water control valves were adjusted throughout the test, if, due to fluctuations in air or water flow, the discharge water temperatures did not remain constant. The water from each section was discharged in separate buckets, and weighed during and/or after each test interval. Temperature

readings of inlet and outlet air and water were taken at five minute intervals as were air volume measurements.

After each test, the valve setting on the discharge end of the equipment was changed to vary the amount of air passing through the test section and thus the test Reynolds Number. Conditions were then allowed to reach equilibrium under the new setting, water flows were again adjusted and the new test carried out. A total of thirty-six tests were carried out over a range of Reynolds Numbers from 1,164 to 135,900.

INSTRUMENTATION

AIR FLOW MEASUREMENT

A number of methods of measuring the air flow were considered. In an attempt to avoid disturbing the air flow before or after the test section, the air flow leaving the compressor and that leaving the by-pass were measured using impact tubes. The difference between these two readings should have represented the volume passing through the test section. This method was not found reliable, as the velocity distribution in the duct ahead of the compression tank was not uniform. This was caused mainly by the centrifugal forces acting on the air passing through the elbows immediately ahead of the plane where the impact

readings were taken. Attempts were made to render the velocity distribution more uniform, by placing turning vanes in the elbows, followed by straightening vanes in the horizontal section of ducting, however, these modifications did not appreciably improve the results.

A method of measuring the air flow through the test section in a positive manner, rather than by difference, was finally adopted. As impact tubes are not reliable at very low velocities such as encountered for the low air flow conditions corresponding to laminar flow, a positive displacement meter was used for the low velocities. Beyond the capacity range of the meter an impact tube was used in conjuntion with a water manometer. To check the accuracy, readings were taken by both methods under flow conditions near the upper limit of the meter capacity, the two methods gave results which compared within three percent. It is estimated that the air flow measurement was accurate within one percent when using the positive displacement meter and within three percent when using the impact tube. The higher inaccuracy when using the impact tube is attributed to the considerable variation in manometer readings during each test.

TEMPERATURE MEASUREMENTS

COOLING WATER

In order to obtain as high a temperature difference as possible between air in the inner pipe and water in the annulus, the inlet water temperature was kept as low as possible by drawing large volumes of water from the main water supply line. As all this water could not be passed through the test equipment, since the water temperature rise would have been too small, a by-pass line was connected from the supply main and directed into a drain.

The cooling water temperature rise was only five to ten degrees, consequently, precision thermometers having an accuracy of one hundredth of a degree were selected for water temperature measurements. Due to variations in temperature readings, it was impossible to read the thermometers to their full accuracy. The estimated error in water temperature readings, based on the temperature rise through the test section was in the order of two percent.

AIR

The inlet air temperature was taken as an average of three thermometer readings, one indicating the tank temperature, another, the by-pass temperature and a third, the temperature in

the jacketed inlet section. Calculations were made for the velocity temperature effect in the by-pass and in the jacketed section; these were found to be in the order of one quarter of one percent of the temperature loss through the test section and, consequently, were neglected. The three inlet temperature thermometers indicated considerable variance, as the tank temperature was always considerably lower than the other two. This difference in temperature may have been due to the high heat loss through the tank wall, which caused a lower temperature at the thermometer well near the wall, than in the main air stream. It is estimated that this variation in inlet temperature may have given results for the heat transfer coefficient which are three percent low at the low air flows, and fifteen percent low at the high air flows.

The discharge temperature was taken a short length after the insulated section, it was measured using an iron constantin thermocouple arranged as shown in Figure 13 in conjunction with a precision potentiometer. This arrangement for the thermocouple was used to obtain a total temperature. The corresponding static temperature was obtained from velocity temperature corrections. Before the test, the thermocouple used was checked against a precision thermometer in a water bath at various temperatures, and was found to give agreement within two percent based on air temperature drop in test section.

WATER FLOW

The cooling water passing through the various sections was collected separately and weighed during or after each test, using a scale having an accuracy of 0.01 pounds in ten pounds, thus giving an accuracy of one tenth of one percent.

PART THREE

RESULTS

CALCULATIONS AND PRESENTATION OF RESULTS

Average values of the test readings and of the calculated results are tabulated in tables II to XVI in the Appendix.

The bases of calculations leading to the tabulated results are outlined below, and a sample calculation is shown in the appendix.

The mass air flow through the test rig was calculated for each test from the measured or calculated volume rate of air flow, by taking into account the temperature and pressure conditions at the discharge of the test rig. The volume flow rates for tests sixteen to thirty-six were calculated from the velocity pressure and temperature readings taken at the rig outlet. For the first fifteen tests the volume flow rates were obtained directly from meter readings. Table IV tabulates the volume and mass flow rates for all tests.

The mass velocity G which is a measure of the mass flow per unit area, was calculated for each test from the mass flow rate and the cross-sectional area of the test section. The Reynolds and Prandtl numbers were evaluated using physical properties of the air at the average temperature of the test section. The inside diameter of the inner test pipe was used as the characteristic dimension in the

calculation of Reynolds numbers. Values of G, N_{Re} and N_{Pr} for each test are tabulated in table VII.

The heat gain from surroundings was established from a heat balance across the test section, from the following relation: Heat from surroundings equals heat gained by water in annulus minus heat loss by air in inner pipe. From the heat gained from surroundings, an overall heat transfer coefficient "U_s" between annulus and surroundings was calculated for each test, based on outer area of outer pipe and arithmetic mean temperature difference between water in the annulus and the space temperature. Values of "U_s" for each test are tabulated in table VI. As the results of the first fifteen tests were more accurate than the latter ones, an average "U_s" based on the first fifteen tests was used as described later to calculate the heat gained from surroundings to each section of the annulus.

An overall heat transfer coefficient "U_a" between the annulus and the inner pipe was calculated using the logarithmic mean temperature difference between the two flowing media. As the inside temperature of the inner pipe was not available from test data, the average heat transfer coefficient "h_a" inside the inner pipe was calculated from the overall heat transfer coefficient "U_a". To enable the calculation of the heat transfer coefficient inside the inner pipe it was necessary to assume a heat transfer coefficient between the inner pipe and the water in the annulus. McAdams [5] states that the

heat transfer coefficients for water vary from 50 to 3000 BTU/hr/ft^2/^{o}F depending on the water velocity. For the nominal water velocity encountered here, a factor of 500 was selected as being representative. The sample calculations show that the results obtained using an "h_w" of 500 differ only by 1% from that obtained using an "h_w" value of 400.

From the calculated values of "h_a" average Nusselt numbers N_{Nu_a} were calculated for each test, based on "K" values corresponding to the average temperature in the test section. The calculated values of U_a, h_a and N_{Nu_a} are tabulated in table IX.

The viscosities μ_b and μ_w were evaluated for each test at the average of inlet and outlet temperatures for air and water respectively. The effect of viscosity on the test results are tabulated in table X and incorporated in the curves plotted on figures 19, 20 and 21.

The temperature drops along length increments of the test section were calculated from water flow rates through the individual sections and from the average overall heat transfer coefficient "U_s" previously referred to. From the temperature drops along the test section, the local heat transfer coefficient "h_x" and the local Nusselt number N_{Nu_x} were calculated for a number of tests, the results of above calculations are tabulated in tables XIII and XV and plotted on curves in figures 22 to 24.

DISCUSSION OF RESULTS

COMPARISON OF RESULTS WITH PUBLISHED DATA

Figures 15 to 25 indicate a comparison of the actual test results with that obtained by other observers.

Figure 16 shows a plot of $N_{Nu}/N_{Pr}^{0.4}$ vs. N_{Re}, solving for the parameters of Equation (27) from the above curve, it can be rewritten as:

$$N_{Nu} = 0.06 \ N_{Re}^{0.69} \ N_{Pr}^{0.4} \quad \text{.....(53)}$$

A similar plot of $N_{Nu}/N_{Pr}^{1/3}$ vs. N_{Re} in Figure 17 gives the following value for the parameters of Equation (27):

$$N_{Nu} = 0.058 \ N_{Re}^{0.69} \ N_{Pr}^{1/3} \quad \text{.....(54)}$$

Comparing Equations (53) and (54) to Equation (45) which is Dittus & Boelter's equation for cooling, the test results are found to give higher values of N_{Nu} at low N_{Re} and lower values of N_{Nu} at high N_{Re} than the Dittus Boelter equation. This is as anticipated, due to the larger errors at the high flow rates, as calculated in the Appendix.

To establish the effect of varying viscosity on Nusselt Number, $N_{Nu}/N_{Pr}^{1/3} (\mu_b/\mu_w)^{0.14}$ was plotted vs. N_{Re} on Figure 19 from which the following equation was found to be represent-

ative of the results obtained.

$$N_{Nu} = 0.060\ N_{Re}^{0.68}\ N_{Pr}^{1/3}\ (\mu_b/\mu_w)^{0.14} \quad \ldots\ldots\ldots\ldots\ldots (55)$$

It can be seen from Figure 19 that the test results give somewhat lower values than predicted by Sieder and Tate in Equation (46).

To compare the results obtained with that predicted by Burbach, Eagle and Ferguson in Equation (47) in which they claim that the Nusselt Number varies as $(D/L)^{1/18}$,

$N_{Nu}/(N_{Pr})^{1/3}\ (\mu_b/\mu_w)^{0.14}\ (D/L)^{1/18}$ was plotted versus N_{Re} in Figure 20. The equation:

$$N_{Nu} = 0.071\ N_{Re}^{0.68}\ N_{Pr}^{1/3}\ (\mu_b/\mu_w)^{0.14}\ (D/L)^{1/18} \quad (56)$$

was found to satisfactorily represent the results obtained. This is seen to give somewhat lower values of N_{Nu} than did Equation (47).

Test results were plotted in Figure 21 in the form of

$N_{St}\ N_{Pr}^{2/3}\ (\mu_w/\mu_b)^{0.14}$ vs. N_{Re} for L/D of 25.

It was established from the resulting curve that the following equation is representative of the results:

$$Y = N_{St}\ N_{Pr}^{2/3}\ (\mu_w/\mu_b)^{0.14} = \frac{0.09}{N_{Re}^{-0.33}} \quad \ldots\ldots\ldots (57)$$

This equation gives slightly higher values except at large N_{Re} than predicted by Colburn in Equation (48).

Upon examining the various data plotted versus N_{Re} it can be noted that the transition from laminar to turbulent flow appears to

begin at about N_{Re} of 3,000. The transition region although not showing a definite break, does appear to end at N_{Re} of about 6,000. The N_{Re} of 3,000 at which the transition region begins is somewhat higher than the normal N_{Re} of 2,300. This may be due to the use of Shelby tubing for the test rig rather than ordinary piping, the tubing being considerably smoother would permit the flow to remain laminar for a longer length, thus causing the transition point to occur at the higher N_{Re}.

To establish the variation of the local heat transfer coefficient within a tube with distance from the tube entrance, Figure 22 was plotted from the calculated value of "h_x" along the tube. It can be seen that for tests 10, 16, 20 and 26 for which the flow was turbulent; the "h_x" is very large at the tube entrance, then decreases very rapidly up to a distance along the tube, equivalent to L/D = 5, and from that point on reduces very slowly. This approaches Deisler's[10] claim that for N_{Pr} = 1 and for high N_{Re} the heating rates reach 99% of the fully developed turbulent value in 5 to 7 diameters. Hartnett[14] claims that for oil and water, the heat transfer coefficient attains a value within 5% of its ultimate value within 2 or 3 diameters. For laminar flow conditions, represented by curves on Figure 22 corresponding to test #1 the local h_x, dropped quickly from a large value at the tube inlet,

then decreased slowly in the direction of flow, but did not reach a constant value within the length of the test section. The local Nusselt Number N_{Nu_x} is found to behave in much the same way as the local heat transfer coefficient, this is shown for conditions of laminar and turbulent flow on curves in Figures 23 and 24 respectively where N_{Nu_x} is plotted vs $\frac{X}{D} \frac{1}{N_{Re} N_{Pr}}$

Unfortunately, the test section was not long enough to achieve a fully established temperature distribution, consequently, it was not possible to verify Giedt's [2] claim that for a uniform wall temperature; the local Nusselt Number normally reaches a constant value of 3.65 when $\frac{X}{D} \frac{1}{N_{Re} N_{Pr}}$ reaches 0.05.

Figure 18 shows a curve of the average heat transfer coefficient "h_a" plotted versus N_{Re}. From the above noted curve, the following equation can be written as being representative of the test results:

$$h_a = 0.0058 \quad N_{Re}^{0.69} \qquad \text{----------(58)}$$

As very few tests were carried out at laminar flow conditions, no specific conclusions can be reached as to the heat transfer characteristics under these conditions. In Figure 25 a few points corresponding to the laminar flow range were plotted as

$$N_{Pe} \text{ versus } N_{Nu_a} (D/L)^{1/3} (\mu_b/\mu_w)^{0.14}$$

yielding the following equation:

$$N_{Nu_a} = 1.82 (N_{Pe})_b^{0.31} (D/L)^{1/3} (\mu_b/\mu_w)^{0.14} \quad \ldots\ldots\ldots\ldots (59)$$

Equation (34) for the laminar flow range is also plotted on Figure 25. It can be seen that the test results are considerably lower than that predicted by Equation (34) for laminar flow conditions.

The above comparison of results with published data by other observers, reveals that the test results are generally low. This discrepancy may be due to various inaccuracies in the testing procedure, or to incorrect assumptions as discussed in the following sections.

EXPLANATION AND DISCUSSION OF ERROR ANALYSES

A calculation of the possible errors in the results is carried out in the Appendix. The various criteria used in the calculation of errors are discussed below.

MASS FLOW

As successive readings at the same point of the impact tube traverse taken at the end of the test rig varied appreciably, some error in the measured flow rates is anticipated. The variations in readings taken as a percentage of the total reading cons-

titute the error in mass flow, which was calculated as ± 3%.

WATER TEMPERATURE RISE

Thermometers having an accuracy of one hundredth of a degree were used for measurement of inlet and outlet water temperatures. All thermometers were immersed in a bath of cold water prior to testing and were found to be accurate within their stated calibration limits. Variations in water temperature conditions limited the reading accuracy to one tenth of a degree. The reading accuracy compared to the temperature rise in the section constitutes the possible error which was calculated as ± 2%.

WATER FLOW

The scale used for weighing the water passing through each section was accurate within one hundredth of a pound, consequently, as the water collected in each bucket per test was approximately ten pounds the inaccuracy in water flow measurements was calculated as ±.1% which is considered negligible.

INLET AIR TEMPERATURE

As stated in pages 52 and 53, the tank temperature was consistently lower than the by-pass and jacket temperatures. The possi-

ble absolute error in inlet air temperature was taken as one half the difference between the tank temperature and an average of the by-pass and jacket temperatures. The absolute error when applied to the temperature drop across the section established the possible percent error, as $\pm$ 11%.

DISCHARGE AIR TEMPERATURE

The accuracy of thermocouple readings using the potentiometer, is limited by the discrepancy in successive readings at a given point in the traverse. This was found to be one half degree, which, applied to the overall temperature drop across the section established the percent accuracy as $\pm$ 2%.

As the temperature was not measured immediately at the end of the test section, in an effort to avoid disturbances in the air stream, the measured temperature would tend to be slightly low. An estimate of the error is made by considering the temperature in the jacket at the end of the test section as being twenty degrees lower than the temperature at the end of the test section. The ratio of the local heat transfer coefficient to the average coefficient, and the ratio of lengths are used to arrive at the possible error in discharge temperature. This was calculated as being one percent low.

Combining, the various possible errors calculated in the

Appendix and noted above it follows that the results should be accurate within twenty percent.

To verify the above noted accuracy the heat gained from surroundings was also calculated from published data. McAdams[5] gives the combined heat gain from surroundings to a pipe at 40° differential from room temperature as 1.84 BTU/hr/ft^2/$^{\circ}$F. The Appendix shows a comparison of the heat from surroundings for various tests, with the calculated values from published data using the above basis. For most tests, the accuracy was found to be within the 20% figure stated above.

EFFECT OF ASSUMED h_w

The Sample Calculation and the Error Analyses in the Appendix illustrate the effect of the assumed value of h_w on the calculated value of h_a. This effect is particularly noticeable at high air flow rates corresponding to high Reynolds Numbers.

It is apparent from the calculation of h_w by two methods as shown in the Appendix, that the value of h_w should have been in the order of 50 rather than 500. The main cause for the low h_w here, is the extremely low velocity through the annulus as compared to that normally encountered in heating applications.

As the error in the calculated h_a gets progressively larger

with increase in flow rate, the net effect is to change the slope of the curves. The above is illustrated in Figure 19 from results calculated using h_w of 50. The resultant curve can be seen to agree very closely with that predicted by Sieder and Tate.

CONCLUSIONS

It is apparent from the discussion of possible errors and the calculation of h_a based on $h_w = 50$ that the discrepancy in the results from that of other observers is mainly attributable to the incorrect assumption for h_w. Figures 18 and 19 illustrate the effect of h_w on the calculated value of h_a particularly at high heat transfer rates.

Revised curves were plotted only for Figures 18 and 19 to point out the effect of the improper assumption, however all curves which include a relation of h_a and N_{Nu_a} would be similarly affected.

SUMMARY

The convective heat transfer inside a tube has been investigated for conditions of laminar and turbulent flow over a Reynolds Number range from 1,164 to 135,900. Thirty-six tests were carried out using air in the inner pipe and water in the annulus of a concentric pipe test rig.

The transition from laminar to turbulent flow conditions was found to occur at a Reynolds Number of approximately 3,000. This is somewhat higher than the normally accepted Reynolds Number of 2,300 at the transition point.

The equations:

$$N_{Nu_a} = 1.82\,(N_{Pe})_b^{0.31}\,(\mu_b/\mu_w)^{0.14}\,(D/L)^{1/3}$$

and

$$N_{Nu_a} = 0.027\,N_{Re}^{0.78}\,N_{Pr}^{0.33}\,(\mu_b/\mu_w)^{0.14}$$

represent the results obtained for the average Nusselt Number at laminar and turbulent flow conditions respectively. These results agree very closely with that predicted by other observers.

The average heat transfer coefficient for a smooth tube having a length to diameter ratio of twenty-five is represented by $h_a = 0.0027\,N_{Re}^{0.78}$ for N_{Re} larger than 3.0×10^3 and by $h_a = 0.28\,N_{Re}^{0.21}$ for N_{Re} less than 3.0×10^3.

The local heat transfer coefficient was found to be very large

at the tube inlet, it then decreased rapidly in the direction of flow up to a length along the tube equal to five diameters, then decreased very slowly along the remaining length of tube.

The tabulated results and the plotted curves were based on an assumed value of $h_w = 500$, this was seen to give low results. When an h_w of 50 was used, results comparable with that of other observers were obtained, these are plotted on Figures 18 and 19.

BIBLIOGRAPHY

BIBLIOGRAPHY

1. Jakob, Max. Heat Transfer, Volume One. John Wiley and Sons 1949

2. Giedt, Warren H. Principles of Engineering Heat Transfer, D. VanNostrand Company Inc., 1957.

3. Kestin J. and Richardson P.D., "Heat Transfer Across Incompressible Boundary Layers". International Journal of Heat and Mass Transfer, February, 1963, pp. 147-186.

4. Eckert, E.R.G. Heat and Mass Transfer, Second Edition, McGraw-Hill Book Company, Inc., 1959.

5. McAdams, William H. Heat Transmission, Third Edition, McGraw-Hill Book Company, Inc., 1954.

6. Eckert, E.R.G. Introduction to the Transfer of Heat and Mass McGraw-Hill Book Company, Inc.

7. Kays, W.M. and Nicoll W.B. "Laminar Flow Heat Transfer to a Gas with Large Temperature Differences", A.S.M.E. Transactions (November, 1963). pp. 329-341.

8. Akins, R.G. and Dranoff, J.S. "Experimental Study of Laminar Flow Heat Transfer with Prescribed Wall Heat Flux" American Institute of Chemical Engineers Journal, Volume 9, Number 5, September, 1963. pp. 624-629.

9 Ermolin, V.K. "Local and Average Heat Transfer Coefficients at an Air Stream in a Tube With a Pointed Inlet", International Journal of Heat and Mass Transfer, 1960. pp. 147-151.

10. Lancet, R.T. "The Effect of Surface Roughness on the Convection Heat Transfer Coefficient for Fully Developed Turbulent Flow in Ducts with Uniform Heat Flux", Transactions of the A.S.M.E., Volume 81, Series C, No. 2, May, 1959. pp. 168-173.

11. Dipprey, D.F. and Sabersky, R.H. "Heat and Momentum Transfer in Smooth and Rough Tubes at Various Prandtl Numbers". International Journal of Heat & Mass Transfer, May, 1963. pp. 329-354.

12. Sabersky, R.H. "Recent Developments in Convective Heat Transfer" A.R.S. Journal 29, n 5, May, 1959, pp. 325-331.

13. Brunello, G and Brun, E. "Contribution a l'étude de la Convection Forcée de la Chaleur sur des Paroies Rugueuses" Publication Scientifiques et Techniques du Ministere de l'Air.

14. Hartnett, J.P. "Experimental Determination of Thermal Entrance Length for the Flow of Water and of Oil in Circular Pipes". A.S.M.E. Transactions , Vol. 77, November, 1955.

APPENDIX

SAMPLE CALCULATIONS

Equipment Dimension Data:

External diameter of inner test pipe = 1.930 in. = 0.161 ft.

Internal diameter at test section = 1.875 in. = 0.1563 ft.

Internal diameter at impact tube = 1.435 in. = 0.1196 ft.

X-sectional area at test section $\frac{\pi \times 0.156^2}{4}$ = 0.0192 ft.^{2}

X-sectional area at impact tube $\frac{\pi \times 0.1196^2}{4}$ = 0.0112 ft.^{2}

Total length of test section = 47.125 in.

Length of test section excluding sections 1 & 13 = 39.625 in.

Inner area of inner pipe $\frac{\pi \times 1.875 \times 47.125}{12 \times 12}$ = 1.933 ft.^{2}

Outer area of inner pipe $\frac{\pi \times 1.930 \times 47.125}{12 \times 12}$ = 1.983 ft.^{2}

Average area of inner pipe $\frac{1.933 + 1.983}{2}$ = 1.958 ft.^{2}

External diameter of outer pipe = 4.25 in.

External area of outer pipe $\frac{\pi \times 4.25 \times 39.625}{12}$ = 3.69 ft.^{2}

All calculations are based on data from test #1 unless otherwise noted.

1. Calculation of Mass Flow W, Mass Velocity G and Reynolds Number N_{Re}.

   As the air flow was measured by two methods, a sample calculation is shown using each method.

(a) Test 1

Air flow was measured directly by meter = 3.3cfm

Air density at outlet $\frac{14.7 \times 144}{53.3 \times 560}$ = 0.0709 lbs/ft.^{3}

Where discharge temperature and pressure are 100^{o}F = 560^{o}R and 14.7 psia respectively.

W = Mass flow = 3.3 x .0709 x 60 = 14.03 lbs/hr.

G = Mass Velocity = 14.03/0.0192 = 0.732 lbs/hr.ft.^{2}

Where: 0.0192 = cross-sectional area at test section

$$N_{Re} = \frac{GD}{\mu}$$

μ is taken at average of inlet and outlet temperatures

Average temperature = $\frac{175.60 + 100.00}{2}$ = 137.8 degree F.

μ at 137.8 degree F = 0.0482 lbs/hr/ft.

$N_{Re} = \frac{0.732 \times 0.1563}{0.0482}$ = 2375

(b) Test 16

Air flow was obtained from impact tube readings using relationship

$$V = \sqrt{\frac{2g\ d_w\ h_v}{12\ d_a}}$$

Where d_w = Water density in the manometer, this was taken as 62.4 lbs/ft^3 for all tests.

The above relation simplifies to $V = 1096.2 \cdot \frac{\sqrt{h_v}}{\sqrt{d_a}}$

where h_v is the manometer reading at the impact tube and d_a is the air density at the impact tube.

For test #16, $d_a = \frac{14.7 \times 144}{53.3 \times (460+138)}$ = 0.0663 lbs/ft/3

$V = \frac{1096.2 \times 0.693}{\sqrt{0.0663}}$ = 2920 ft/min.

$Q = AV$

$= .0112 \times 2920$ = 32.7 cfm

where 0.0112 = cross-sectional area at impact tube.

W = Mass Flow = $32.7 \times 60 \times 0.0663$ = 130.0 lbs/hr.

Average air temperature in test section = $\frac{177.2 + 138.0}{2} = 157.6^{\circ}F$

Viscosity μ at 157.6 degree F - = 0.0494 lbs/hr/ft.

G = Mass Velocity = $\frac{130.0}{0.0192}$ = 6780 lbs/hr/ft^2

$N_{Re} = \frac{GD}{\mu} = \frac{6780 \times .1563}{0.0494}$ = 21,440

2. Heat Gained by Water

The water flow through sections 1 and 13 were omitted as these sections had an extremely high heat gain from the end section.

Test #1 - Water flow through sections 2 - 12 inclusive for 30 minute test = 80.10 lbs. i.e. 160.20 lbs/hr.

Water temperature rise = 4.4 degree F.

Heat picked up by water 160.20×4.4 = 705.0 BTU/hr.

3. Heat loss by Air in Inner Pipe

Mass flow test #1 = 14.03 lbs/hr.

Temperature drop through test section = 75.2 degree F.

Heat loss by air = $14.03 \times 75.2 \times 0.241$ = 255 BTU/hr

4. Heat Gained From Surroundings

The difference between heat picked up water and heat loss by air in the inner pipe can only be attributable to heat gain from surroundings which

for test #1 = 705.0 - 255.0 - 450.0 BTU/hr

5. L.M.T.D. between air in the inner pipe and water in the annulus.

$$L.M.T.D. = \frac{(\Delta T \text{ hot}) - (\Delta T \text{ cold})}{\ln(\Delta T \text{ hot}) / (\Delta T \text{ cold})}$$

Where ΔT hot = Air inlet temperature - water outlet temperature

ΔT cold = Air outlet temperature - water inlet temperature

Test #1

$$\Delta Tm = L.M.T.D. = \frac{(175.60 - 45.0) - (100.0 - 40.6)}{\ln(130.25/59.4)} =$$

$$\frac{70.8}{0.786} = 90.2^{\circ}F$$

6. Average Overall Heat Transfer Coefficient U_a

U_a between air in the inner pipe and water in the annulus, is based on the average area of the inner pipe = 1.958 ft^2

$$U_a = \frac{\text{Heat from air}}{A \quad \Delta Tm} = \frac{255}{1.958 \times 90.2} = 1.45 \text{ BTU/hr/ft}^2/^{\circ}F.$$

7. Average Heat Transfer Coefficient h_a

The overall coefficient calculated in item 6 is based on the resistance in going through the tube wall and through film coefficients on both sides of the wall. i.e.,

$$U_a = \frac{1}{\frac{1}{h_w} + \frac{x}{K} + \frac{1}{h_a}}$$

(a) Where h_w = heat transfer coefficient in the annulus, assume value of 500 BTU/hr/$ft^2/^{\circ}F$.

x = thickness of tube wall = 0.125 inches.

k = thermal conductivity of the wall = 300.

h_a = heat transfer coefficient in the inner pipe.

$$U_a = \frac{1}{\frac{1}{500} + \frac{0.125}{300} + \frac{1}{h_a}} = \frac{1}{0.002 + 0.0004 + \frac{1}{h_a}}$$

which simplifies to: $\frac{1}{h_a} = \frac{1}{U_a} - 0.0024$

For test #1

$$\frac{1}{h_a} = \frac{1}{1.45} - 0.0024 = 0.687$$

$$h_a = 1.46 \text{ BTU/hr/ft}^2/^\circ\text{F}$$

For test #31

$$\frac{1}{h_a} = \frac{1}{U_a} - 0.0024$$

$$\frac{1}{h_a} = \frac{1}{20.40} - 0.0024 = 0.04662$$

$$h_a = 21.45$$

(b) Check effect on h_a if h_w assumed as 400

$$\frac{1}{h_a} = \frac{1}{U_a} - \left(\frac{1}{400} + 0.0004\right)$$

$$= \frac{1}{U_a} - (0.0025 + 0.0004) = \frac{1}{U_a} - 0.0029$$

For test #1

$$\frac{1}{h_a} = \frac{1}{1.45} - 0.0029 = 0.6871$$

$$h_a = 1.46$$

For test #31

$$\frac{1}{h_a} = \frac{1}{20.40} - 0.0029 = 0.0461$$

$$h_a = 21.7$$

NOTE: This is only 1.1% higher than for $h_w = 500$

(c) Check effect on h_a if h_w assumed at 100

$$\frac{1}{h_a} = \frac{1}{U_a} - (0.01 + 0.0004) = \frac{1}{U_a} - 0.0104$$

For test #1

$$\frac{1}{h_a} = \frac{1}{1.45} - 0.0104 = 0.6796$$

h_a = 1.47 which is within 1% of h_a based on h_w = 500

For test #31

$$\frac{1}{h_a} = \frac{1}{20.40} - 0.0104 = 0.0386$$

h_a = 25.9

NOTE: This is 19.2% higher than for h_w = 500

(d) Calculation for h_a based on wall temperature equal to average water temperature

For test #1

Average water temperature = 42.8°F

Average air temperature = 137.8°F

$Q = h_a \ A\Delta T$

$255.0 = h_a \times 1.958 \ (137.8 - 42.8)$

$h_a = \frac{255.0}{1.958 \times 95.0}$ = 1.37 which is 7% lower than when h_w = 500 was assumed.

For test #31

Average water temperature = 44.75°F

Average air temperature = 167.10°F

$h_a = \frac{4870}{1.958 \times (167.10 - 44.75)}$ = 20.30

NOTE: That this result is also 7% lower than when $h_w = 500$ was assumed.

8. Calculation of overall heat transfer coefficient U_s between the annulus and surroundings.

For test #1

Heat gain from surroundings = 450 BTU/hr

Temperature difference = room temperature - average water temperature

$= 75.2 - 42.8 = 32.4^{\circ}F$

Area $= 3.69\ ft^2$

$Q = U_s\ A\Delta T$

$U_s = 450/3.69 \times 32.4 = \underline{3.77\ BTU/hr/ft^2/^{\circ}F}$

9. Calculation of Prandtl Number N_{Pr}

$N_{Pr} = C_p\ \mu/K$

$C_p = 0.241$ for all tests

μ and K, evaluated at average air temperature are 0.0482 and 0.0166 respectively.

For test #1

$N_{Pr} = 0.241 \times 0.0482/0.0166 = \underline{0.700}$

10. Calculation of average Nusselt Number N_{Nu_a}

$N_{Nu_a} = h_a D/K$

where D = inside diameter of test section = $0.1563\ ft^2$

For test #1

$N_{Nu_a} = 1.45 \times 0.1563/0.0166 = \underline{13.70}$

11. Calculation of the local heat transfer coefficient h_x along the tube length

For test #1. Section 12

To establish the heat gain from the surroundings to each section of the annulus, the average value of the calculated U_s (item 8) was obtained from the results of the first fifteen tests. This average value of U_s was 3.95 BTU/hr/ft^2/$^\circ$F. Water collected in section 13 (from test data) = 5.67 lbs. in 30 min. or 11.34 lbs/hr.

Temperature rise in cooling water = 4.4°F (from test data)

Heat picked up by water = 11.34 x 4.4 = 51.02 BTU/hr

Area of the section exposed to surroundings = $\frac{4.25}{12} \times \frac{1}{12}$ = 0.0927 ft^2

Temperature differential between annulus and surroundings = 32.4°F (see item 8)

Heat picked up from surroundings = 3.95 x 0.0927 x 32.4 = 11.84 BTU/hr

Heat picked up from air = 51.02 - 11.84 = 39.18 BTU/hr

Air flow for test #1 (see item I) = 14.03 lbs/hr

From relation : $Q = WC_p \Delta T$ the temperature drop in the specific section is calculated:

$$\Delta T = \frac{Q}{WC_p} = \frac{39.18}{14.03 \times 0.241} = 11.65^\circ F$$

From the calculated temperature drops along the test length, the temperature at any point along the pipe is calculated. Based on the air temperature inside the pipe and the average annulus water temperature, an average local overall coefficient of heat transfer is calculated.

$$U = \frac{39.18}{\text{Area} \times \text{Temperature difference}}$$

$$\text{Area} = \pi \times \frac{1.90}{12} \times \frac{1}{12} = 0.0415 \text{ ft}^2$$

where 1.90 in. = average diameter of inner pipe

1 in. = length of section 12

Temperature difference = 124.2°F based on difference between annulus temperature and calculated temperature inside inner pipe.

$$U = \frac{39.18}{0.0415 \times 124.2} = 7.6 \text{ BTU/hr/ft}^2/^\circ\text{F}$$

h_x is calculated as shown for h_a (item 7) assuming a value of h_w = 500

$$\frac{1}{h_x} = \frac{1}{U} - 0.0028 = \frac{1}{7.6} - 0.0028 = 0.1289$$

$h_x = \underline{7.77 \text{ BTU/hr/ft}^2/^\circ\text{F}}$

From the local h_x the local N_{Nu_x} is calculated, based on the K value at the calculated temperature within the section.

TABLE II

TEST DATA

Test No.	Room Temp. °F	Inlet Water Temp. °F	Outlet Water Temp. °F.	Inlet Air Temp. °F.	Outlet Air Temp. °F.
1	75.2	40.6	45.0	175.6	100.0
2	75.4	40.8	45.0	175.2	115.3
3	76.5	39.0	43.0	173.8	90.0
4	78.9	39.1	44.2	175.9	115.2
5	78.2	38.8	44.1	177.9	122.4
6	80.0	39.1	44.9	180.7	128.5
7	77.8	38.4	43.2	173.5	128.3
8	78.1	38.2	43.0	176.7	131.9
9	79.9	39.1	44.0	173.9	132.1
10	80.5	39.1	44.0	174.0	131.0
11	80.8	39.2	44.0	175.9	130.5
12	80.7	39.1	44.0	172.8	127.3
13	76.6	41.0	46.3	173.2	75.4
14	79.7	39.1	45.1	176.0	119.4
15	81.5	39.0	45.2	177.5	123.8
16	82.2	38.9	44.9	177.2	138.0
17	80.6	38.9	44.8	181.6	147.3
18	80.1	38.6	47.2	181.7	149.1
19	81.3	39.0	47.1	179.0	149.1
20	81.6	39.0	50.1	181.9	153.5
21	75.0	39.4	44.8	176.8	129.8
22	75.2	39.1	44.9	181.9	139.1
23	77.9	39.0	49.8	182.2	154.7
24	76.8	38.3	50.1	179.4	152.6
25	77.5	38.4	50.2	183.8	157.3
26	75.3	39.5	50.2	178.9	153.4
27	74.9	39.5	49.8	176.2	154.5
28	75.1	39.7	50.1	176.6	153.6
29	76.3	39.5	49.9	174.9	154.5
30	76.5	39.2	50.1	180.1	156.5
31	78.3	39.4	50.1	178.0	153.3
32	81.0	39.5	50.0	181.3	157.7
33	81.0	39.5	50.0	178.9	156.7
34	81.2	39.4	49.8	181.7	155.4
35	81.3	39.0	50.0	180.5	154.8
36	80.4	39.1	50.0	176.7	151.0

TABLE III

WATER COLLECTED IN EACH SECTION*

Test No.	Section Number 1	2	3	4	5	6
1	14.68	8.00	7.76	8.36	8.99	8.00
2	17.00	9.83	8.17	10.98	10.29	9.18
3	14.75	8.09	7.56	9.51	10.12	9.27
4	16.00	8.75	7.65	9.16	9.23	8.14
5	15.50	9.49	8.17	9.86	8.86	8.39
6	17.00	10.00	8.91	10.20	10.30	8.70
7	24.50	13.84	11.22	13.79	13.50	14.68
8	25.50	16.12	14.94	14.92	14.84	14.55
9	28.00	17.58	13.05	17.53	14.78	15.81
10	30.00	16.43	13.02	14.40	14.82	14.92
11	27.00	15.58	12.51	14.17	14.06	14.14
12	23.00	14.15	11 .44	13.16	12.58	13.74
13	11.50	6.50	6.77	7.10	7.19	6.37
14	12.50	8.50	7.21	8.04	7.65	7.14
15	16.00	9.10	9.39	9.16	8.85	7.73
16	17.50	12.29	10.03	10.08	11. 48	9.14
17	23.50	19.84	17.30	17.12	18.46	12.61
18	19.50	14.06	13.83	13.79	12.91	12.72
19	18.50	18.44	15.92	15.97	13.46	14.67
20	17.50	13.64	12.44	13.42	13.11	1 1.32
21	16.00	9.42	9.39	8.71	8.22	9.03
22	15.50	9.95	10.79	9.61	9.00	9.20
23	18.50	16.05	14.05	15.12	13.30	13.02
24	17.50	15.67	14.11	15.00	14.07	12.62
25	19.50	16.76	15.38	15.62	14.97	14.02
26	21.50	17.90	15.88	19.21	15.63	15.36
27	22.50	19.94	17.57	19.57	17.53	16.35
28	22.50	20.52	17.03	18.50	16.76	16.86
29	22.00	21.33	17.84	19.64	18.51	17.39
30	23.00	22.46	17.52	20.00	18.00	16.62
31	22.50	20.54	18.02	19.58	17.51	16.50
32	22.20	20.67	15.11	19.66	17.69	16.78
33	21.00	20.40	16.79	18.73	16.54	16.13
34	20.50	17.53	15.79	18.03	15.20	14.61
35	19.50	16.55	14.51	15.12	14.18	12.87
36	18.00	14.51	13.30	14.21	13.17	11.62

*All weights in pounds

TABLE III Continued -

WATER COLLECTED IN EACH SECTION *

Test No.	Section Number 7	8	9	10	11	12	13
1	7.70	6.79	7.40	5.73	5.70	5.67	30.74
2	8.61	7.43	8.72	7.66	7.08	6.34	33.05
3	8.04	7.38	8.39	7.48	6.48	5.50	38.25
4	7.43	6.65	7.76	6.38	5.94	5.27	31.25
5	7.60	7.31	7.79	7.02	6.23	5.26	29.25
6	8.30	8.23	8.39	7.18	6.84	5.56	27.50
7	11.76	10.19	10.18	8.92	8.44	5.71	36.00
8	12.75	10.99	11.47	9.52	9.55	5.99	35.50
9	13.61	12.94	12.26	9.56	10.43	6.29	34.50
10	13.09	10.72	11.51	9.82	9.25	6.25	35.00
11	13.00	10.55	11.27	9.76	9.09	6.23	35.50
12	11.48	9.70	10.46	8.37	7.78	5.50	33.00
13	5.90	5.34	5.88	4.85	4.42	4.73	29.00
14	7.27	6.16	6.80	5.46	5.35	4.78	26.50
15	7.25	7.32	7.36	6.70	6.03	5.43	26.50
16	9.91	6.91	9.17	6.25	6.58	5.34	20.00
17	13.86	12.30	14.36	9.75	10.94	5.93	26.00
18	11.41	9.82	9.57	8.03	8.35	5.29	18.00
19	12.57	11.60	12.23	8.74	9.74	5.37	19.00
20	10.35	8.91	9.67	6.45	7.49	4.75	13.00
21	8.73	6.58	7.75	6.53	5.80	3.45	20.50
22	7.82	7.37	7.05	6.38	6.83	4.00	22.50
23	12.35	10.28	10.89	7.63	7.79	5.28	14.00
24	12.14	10.44	11.67	7.38	8.70	5.24	13.00
25	12.16	11.41	11.96	7.61	8.81	5.43	13.00
26	13.22	13.44	13.31	8.88	9.29	5.87	13.00
27	14.93	14.20	13.69	9.52	10.65	6.34	14.20
28	14.05	14.23	13.91	9.55	10.61	6.33	14.20
29	14.43	14.05	13.93	9.54	10.83	6.51	14.20
30	14.92	14.82	13.56	9.34	11.32	6.18	15.50
31	14.48	14.34	13.63	9.36	10.50	6.09	14.50
32	14.83	14.17	13.96	9.70	12.04	6.30	15.00
33	13.98	13.41	13.68	9.43	10.10	6.18	15.00
34	11.92	12.65	12.52	8.07	9.06	5.54	15.50
35	11.66	10.83	11.23	7.67	8.16	5.49	13.20
36	10.76	9.75	9.91	6.91	8.14	5.10	13.40

* All weights in pounds

TABLE IV

RATE OF AIR FLOW

Test No.	$\sqrt{hv}$	da lbs/ft^3	$\sqrt{da}$	V ft/min.	Q cfm	W lbs/hr
1	*	0.0709	*	*	3.30	14.0
2		.0692			5.00	20.9
3		.0722			1.58	6.8
4		.0692			5.56	23.0
5		.0682			7.98	32.6
6		.0675			12.34	50.0
7		.0675			14.93	60.4
8		.0672			20.13	81.1
9		.0672			24.55	98.8
10		.0673			21.60	87.1
11		.0673			18.47	74.5
12		.0677			15.23	61.9
13		.0743			1.90	8.5
14		.0687			6.81	28.0
15		.0681			10.02	41.0
16	0.693	.0663	0.258	2,920	32.70	130.0
17	1.471	.0653	.256	6,210	69.70	272.5
18	1.745	.0652	.256	7,480	83.90	327.0
19	2.033	.0652	.256	8,720	97.80	382.0
20	2.395	.0647	.254	10,300	115.40	448.0
21	0.045	.0674	.260	1,902	21.30	86.1
22	0.559	.0663	.258	2,360	26.40	104.9
23	2.955	.0645	.254	12,730	142.70	552.0
24	3.365	.0647	.254	14,490	162.10	628.0
25	3.445	.0642	.253	14,860	166.30	642.0
26	3.805	.0646	.254	16,400	183.60	710.0
27	3.961	.0645	.254	17,100	191.60	740.0
28	4.170	.0645	.254	17,990	201.30	778.0
29	4.270	.0643	.254	18,410	206.10	795.0
30	4.490	.0642	.253	19,400	217.20	837.0
31	4.390	.0645	.254	18,920	212.20	820.0
32	3.990	.0641	.253	17,250	193.20	743.0
33	3.730	.0642	.253	16,110	180.40	694.0
34	3.205	.0645	.254	13,830	155.00	600.0
35	2.935	.0643	.254	12,640	141.70	546.0
36	2.555	0.0650	0.255	10,980	122.80	479.0

* For tests 1 to 15 inclusive, air flow was measured using a positive displacement meter, therefore, items marked * were not required for air flow calculation.

TABLE V

HEAT LOSS BY AIR

Test No.	Water Flow lbs/hr	Water Temp. Rise °F	Heat to Water BTU/hr	Air Flow lbs/hr	Air Temp. Drop °F	Heat Loss By Air BTU/hr
1	160.20	4.4	705.0	14.0	75.6	255.0
2	188.60	4.2	793.0	20.9	60.0	302.0
3	175.64	4.0	702.6	6.8	83.8	138.0
4	164.72	5.1	840.1	23.0	60.7	337.5
5	169.96	5.3	900.8	32.6	55.5	435.0
6	185.22	5.8	1,074.0	50.0	52.2	629.0
7	244.46	4.8	1,175.0	60.4	45.2	657.5
8	271.28	4.8	1,300.0	81.1	44.8	875.0
9	287.68	4.9	1,408.0	98.8	41.8	997.0
10	276.46	4.9	1,355.0	87.1	43.0	902.0
11	260.72	4.8	1,252.0	74.5	45.4	814.0
12	236.72	4.9	1,155.0	61.9	45.5	628.0
13	130.10	5.3	690.0	8.5	97.8	199.6
14	148.72	6.0	893.0	28.0	56.6	381.5
15	168.64	6.2	1,044.0	41.0	53.7	531.0
16	231.54	6.0	1,749.0	130.0	39.2	1,229.0
17	448.41	5.9	2,642.0	272.5	34.3	2,250.0
18	359.34	8.6	3,090.0	327.0	32.6	2,572.0
19	416.10	8.1	3,365.0	382.0	29.9	2,765.0
20	334.65	11.6	3,720.0	448.0	28.4	3,065.0
21	250.80	5.4	1,356.0	86.1	47.0	976.0
22	264.00	5.8	1,530.0	104.9	42.8	1,084.0
23	377.00	10.8	4,070.0	552.0	27.5	3,660.0
24	381.00	11.8	4,490.0	628.0	26.8	4,070.0
25	402.70	11.8	4,750.0	642.0	26.5	4,110.0
26	443.00	10.7	4,740.0	710.0	25.5	4,370.0
27	480.50	10.3	4,950.0	740.0	21.7	3,860.0
28	475.00	10.4	4,940.0	778.0	22.9	4,300.0
29	492.00	10.4	5,120.0	795.0	20.3	3,895.0
30	494.00	10.9	5,380.0	837.0	23.6	4,760.0
31	482.00	10.7	5,165.0	820.0	24.7	4,870.0
32	482.50	10.5	5,060.0	743.0	23.6	4,230.0
33	466.00	10.5	4,890.0	694.0	22.2	3,710.0
34	422.50	10.4	4,400.0	600.0	26.3	3,760.0
35	386.00	11.0	4,240.0	546.0	25.7	3,380.0
36	352.00	10.9	3,840.0	479.0	25.6	2,950.0

TABLE VI

HEAT GAINED FROM SURROUNDINGS

Test No.	Temp. Diff. °F	Heat To Water BTU/hr	Heat Loss By Air BTU/hr	Heat From Surr. BTU/hr	Average U to Surr. BTU/hr/°F/ft^2
1	32.4	705.0	255.0	450.0	3.77
2	32.5	793.0	302.0	491.0	4.10
3	35.5	702.6	138.0	564.6	4.31
4	37.2	840.1	337.5	502.6	3.66
5	36.8	900.8	435.0	465.8	3.43
6	38.0	1,074.2	629.0	445.2	3.18
7	37.0	1,175,0	657.5	517.5	3.79
8	37.5	1,300.0	875.0	425.0	3.08
9	38.4	1,408.0	997.0	411.0	2.90
10	39.0	1,355.0	902.0	453.0	3.15
11	39.2	1,252.0	814.0	438.0	3.03
12	39.1	1,155.0	628.0	527.0	3.65
13	32.9	690.0	199.6	490.4	4.05
14	37.6	893.0	381.5	511.5	3.70
15	39.4	1,044.0	531.0	514.0	3.55
16	40.3	1,749.0	1,229.0	520.0	3.54
17	38.7	2,642.0	2,250.0	392.0	2.75
18	37.2	3,090.0	2,572.0	518.0	3.77
19	38.2	3,365.0	2,765.0	600.0	4.24
20	36.6	3,720.0	3,065.0	655.0	4.78
21	32.9	1,356.0	976.0	380.0	3.13
22	33.1	1,530.0	1,084.0	446.0	3.65
23	33.5	4,070.0	3,660.0	410.0	3.32
24	32.6	4,490.0	4,070.0	420.0	3.48
25	33.2	4,750.0	4,110.0	640.0	5.25
26	30.4	4,740.0	4,370.0	370.0	3.30
27	33.2	4,950.0	3,860.0	1,090.0	9.75
28	30.2	4,940.0	4,300.0	640.0	5.79
29	31.8	5,120.0	3,895.0	1,225.0	10.50
30	31.8	5,380.0	4,760.0	620.0	5.22
31	33.6	5,165.0	4,870.0	295.0	2.38
32	35.3	5,060.0	4,230.0	830.0	6.38
33	36.3	4,890.0	3,710.0	1,170.0	8.73
34	36.6	4,400.0	3,760.0	640.0	4.72
35	36.8	4,240.0	3,380.0	860.0	6.32
36	35.8	3,840.0	2,950.0	890.0	6.74

TABLE VII

REYNOLDS AND PRANDTL NUMBERS

Test No.	Ave. Temp. °F	Ave. μ_b lb/hr/ft	Ave. K_b BTU hr/ft/°F	Mass Vel. G lbs/hr/ft^2	N_{Re}	N_{Pr}
1	137.8	0.0482	0.0166	732	2,375	0.700
2	145.2	.0486	.0168	1,090	3,500	.697
3	131.9	.0479	.0164	356	1,164	.705
4	145.5	.0486	.0168	1,200	3,860	.698
5	150.2	.0489	.0169	1,700	5,435	.698
6	154.6	.0490	.0170	2,606	8,330	.695
7	150.9	.0489	.0169	3,150	10,070	.697
8	154.3	.0492	.0170	4,230	13,470	.697
9	153.0	.0492	.0170	5,150	16,400	.697
10	152.5	.0491	.0169	4,540	14,470	.699
11	153.2	.0492	.0170	3,890	12,380	.697
12	150.1	.0490	.0169	3,222	10,310	.699
13	124.3	.0475	.0163	441	1,450	.703
14	147.7	.0489	.0169	1,462	4,680	.697
15	150.6	.0490	.0169	2,135	6,830	.699
16	157.6	.0494	.0171	6,780	21,440	.695
17	164.6	.0498	.0173	14,220	44,700	.697
18	165.6	.0499	.0173	17,060	53,500	.695
19	164.4	.0498	.0173	19,940	62,700	.696
20	168.1	.0500	.0174	23,380	73,200	.695
21	153.3	.0492	.0170	4,490	14,300	.698
22	160.5	.0496	.0172	5,470	17,230	.697
23	169.1	.0501	.0174	28,800	90,100	.695
24	166.8	.0500	.0173	32,750	1 02,400	.696
25	171.4	.0502	.0174	33,500	104,300	.695
26	167.2	.0500	.0173	37,000	115,800	.696
27	166.5	.0500	.0173	38,600	121,000	.697
28	166.3	.0500	.0173	40,600	127,600	.697
29	165.2	.0499	.0173	41,400	130,000	.696
30	169.8	.0502	.0174	43,600	135,900	.696
31	167.1	.0500	.0173	42,700	133,500	.698
32	170.7	.0503	.0174	38,700	120,200	.696
33	168.9	.0501	.0174	36,150	112,800	.695
34	169.3	.0501	.0174	31,300	97,800	.695
35	168.3	.0501	.0174	28,500	88,900	.695
36	164.4	0.0499	0.0173	24,900	78,200	0.697

TABLE VIII

CALCULATED RESULTS FROM TEST DATA

Test No.	N_{Re}	$N_{Pr}^{0.4}$	$N_{Pr}^{1/3}$	N_{Nua}	$\frac{N_{Nua}}{N_{Pr}^{0.4}}$	$\frac{N_{Nua}}{N_{Pr}^{1/3}}$
1	2,375	0.867	0.888	13.7	15.8	15.4
2	3,500	.864	.888	14.5	16.8	16.3
3	1,164	.868	.890	8.1	9.4	9.1
4	3,860	.866	.887	15.9	18.4	17.9
5	5,435	.866	.887	19.4	22.4	21.9
6	8,330	.864	.886	27.0	31.2	30.5
7	10,070	.864	.888	28.7	33.2	32.4
8	13,470	.864	.888	36.9	42.8	41.7
9	16,400	.864	.888	42.8	49.7	48.3
10	14,470	.866	.888	39.1	45.2	44.1
11	12,380	.864	.888	35.7	41.3	41.3
12	10,310	.866	.888	29.0	33.5	32.7
13	1,450	.868	.889	14.0	16.2	15.7
14	4,680	.864	.888	17.4	20.2	19.6
15	6,830	.866	.888	23.9	27.6	26.9
16	21,440	.864	.886	51.1	59.2	57.7
17	44,700	.864	.888	87.8	101.9	98.9
18	53,500	.864	.886	101.0	116.3	114.0
19	62,700	.865	.886	110.6	127.9	124.9
20	73,200	.864	.886	120.5	139.4	136.0
21	14,300	.866	.887	42.4	48.9	47.8
22	17,230	.864	.888	43.6	50.5	49.1
23	90,100	.864	.886	141.0	162.4	159.1
24	102,400	.865	.886	164.1	190.0	185.2
25	104,300	.864	.886	153.3	177.1	173.0
26	115,800	.865	.886	174.5	201.5	197.0
27	121,000	.864	.888	153.2	177.5	172.5
28	127,600	.864	.888	174.0	201.2	196.0
29	130,000	.865	.886	155.4	179.8	175.5
30	135,900	.865	.886	183.3	212.0	207.0
31	133,500	.866	.887	195.8	225.9	220.5
32	120,200	.865	.886	162.0	187.4	182.9
33	112,800	.864	.886	142.7	165.2	161.0
34	97,800	.864	.886	144.5	167.2	163.0
35	88,900	.864	.886	134.0	155.2	151.1
36	78,200	0.864	0.888	122.0	141.3	137.4

TABLE IX

AVERAGE HEAT TRANSFER COEFFICIENT
AND AVERAGE NUSSELT NUMBER

Test No.	LMTD ^{o}F	Heat From Air BTU/hr	U_a $\frac{BTU}{hr/ft^2/^{o}F}$	h_a $\frac{BTU}{hr/ft^2/^{o}F}$	K $\frac{BTU}{hr/ft/^{o}F}$	N_{Nu_a} $\frac{h_aD}{K}$
1	90.2	255.0	1.45	1.46	0.0166	13.70
2	99.5	302.0	1.55	1.56	.0168	14.50
3	84.7	138.0	.83	.85	.0164	8.13
4	101.3	337.5	1.70	1.71	.0168	15.90
5	106.8	435.0	2.08	2.09	.0169	19.40
6	110.7	629.0	2.90	2.92	.0170	27.00
7	110.7	657.5	3.08	3.11	.0169	28.70
8	112.7	875.0	3.97	4.02	.0170	36.90
9	110.7	997.0	4.60	4.66	.0170	42.80
10	110.1	902.0	4.20	4.25	.0169	39.10
11	110.4	814.0	3.85	3.89	.0170	35.70
12	107.1	628.0	3.11	3.14	.0169	29.00
13	70.8	199.6	1.45	1.46	.0163	14.00
14	103.4	381.5	1.88	1.89	.0169	17.42
15	106.0	531.0	2.57	2.59	.0169	23.90
16	113.6	1,229.0	5.52	5.60	.0171	51.10
17	121.6	2,250.0	9.45	9.70	.0173	87.80
18	121.0	2,572.0	10.83	11.19	.0173	101.00
19	121.8	2,765.0	11.60	12.22	.0173	110.60
20	125.0	3,065.0	12.55	13.40	.0174	120.50
21	109.8	976.0	4.54	4.62	.0170	42.40
22	117.4	1,084.0	4.72	4.79	.0172	43.60
23	124.1	3,660.0	15.08	15.72	.0174	141.00
24	120.0	4,070.0	17.32	18.20	.0173	164.10
25	129.3	4,110.0	16.28	17.08	.0174	153.30
26	121.6	4,370.0	18.38	19.35	.0173	174.50
27	121.3	3,860.0	16.22	17.00	.0173	153.20
28	119.8	4,300.0	18.34	19.30	.0173	174.00
29	121.1	3,895.0	16.43	17.22	.0173	155.40
30	126.0	4,760.0	19.30	20.40	.0174	183.30
31	122.0	4,870.0	20.40	21.45	.0173	195.80
32	125.6	4,230.0	17.20	18.05	.0174	162.00
33	124.6	3,710.0	15.20	15.89	.0174	142.70
34	125.0	3,760.0	15.38	16.10	.0174	144.50
35	122.7	3,380.0	14.09	14.90	.0174	134.00
36	120.0	2,950.0	12.54	13.48	0.0173	122.00

TABLE X

VISCOSITY FACTOR

Test No.	μ_b lb/hr/ft	μ_w lb/hr/ft	μ_b/μ_w	$(\mu_b/\mu_w)^{0.14}$	$(\mu_w/\mu_b)^{0.14}$
1	0.0482	0.0425	1.132	1.018	0.984
2	.0486	.0425	1.142	1.019	.982
3	.0479	.0426	1.123	1.016	.986
4	.0486	.0426	1.140	1.019	.982
5	.0489	.0426	1.146	1.019	.981
6	.0490	.0426	1.150	1.020	.980
7	.0489	.0425	1.150	1.020	.980
8	.0492	.0425	1.156	1.021	.979
9	.0492	.0426	1.154	1.020	.979
10	.0491	.0426	1.152	1.020	.979
11	.0492	.0426	1.153	1.020	.979
12	.0490	.0426	1.150	1.020	.980
13	.0475	.0427	1.112	1.015	.987
14	.0489	.0426	1.147	1.019	.981
15	.0490	.0426	1.150	1.020	.980
16	.0494	.0426	1.160	1.021	.978
17	.0498	.0426	1.170	1.022	.977
18	.0499	.0427	1.168	1.022	.977
19	.0498	.0427	1.168	1.022	.977
20	.0500	.0427	1.170	1.022	.977
21	.0492	.0426	1.154	1.020	.979
22	.0496	.0426	1.164	1.022	.978
23	.0501	.0427	1.173	1.023	.977
24	.0500	.0427	1.170	1.022	.977
25	.0502	.0427	1.176	1.030	.972
26	.0500	.0427	1.170	1.022	.977
27	.0500	.0427	1.170	1.022	.977
28	.0500	.0427	1.170	1.022	.977
29	.0499	.0427	1.168	1.022	.977
30	.0502	.0427	1.176	1.029	.972
31	.0500	.0427	1.170	1.022	.977
32	.0501	.0427	1.173	1.023	.977
33	.0501	.0427	1.173	1.023	.977
34	.0501	.0427	1.173	1.023	.977
35	.0501	.0427	1.173	1.023	.977
36	0.0499	0.0427	1.168	1.020	0.977

TABLE XI

CALCULATED RESULTS FROM TEST DATA

Test No.	$\frac{N_{Nu}}{N_{Pr}^{1/3}(\mu_b/\mu_w)^{0.14}}$	$\frac{N_{Nu}}{N_{Pr}^{1/3}(\mu_b/\mu_w)^{0.14}(D/L)^{1/18}}$
1	15.2	18.2
2	16.0	19.2
3	9.0	10.7
4	17.6	21.1
5	21.5	25.7
6	29.9	35.8
7	31.8	38.1
8	40.8	48.8
9	47.3	56.7
10	43.2	51.7
11	40.6	48.6
12	32.0	38.3
13	15.5	18.5
14	19.3	23.1
15	26.4	30.4
16	56.6	67.7
17	96.7	115.7
18	111.3	133.3
19	122.0	145.9
20	133.0	159.0
21	46.9	56.2
22	48.0	57.3
23	155.5	185.5
24	181.2	217.0
25	168.0	201.0
26	192.5	230.0
27	168.8	201.5
28	191.5	229.0
29	171.8	205.0
30	201.3	240.0
31	214.5	257.0
32	178.5	213.0
33	157.5	188.2
34	159.5	190.6
35	147.7	176.5
36	134.9	161.0

TABLE XII

CALCULATED RESULTS FROM TEST DATA

Test No.	N_{Re}	N_{Nu}	$N_{Pr}N_{Re}$	N_{St}	$N_{Pr}^{2/3}$	$N_{St}\,N_{Pr}^{2/3} \times (\mu_w/\mu_b)^{0.14}$
1	2,375	13.70	1,660	0.00820	0.976	0.00786
2	3,500	14.50	2,438	.00595	.976	.00569
3	1,164	8.13	822	.00990	.977	.00952
4	3,860	15.90	2,695	.00591	.976	.00565
5	5,435	19.40	3,792	.00512	.976	.00489
6	8,330	27.00	5,780	.00467	.976	.00446
7	10,070	28.70	7,005	.00410	.976	.00391
8	13,470	36.90	9,380	.00394	.976	.00376
9	16,400	42.80	11,420	.00374	.976	.00357
10	14,470	39.10	10,100	.00387	.977	.00369
11	12,380	35.70	8,630	.00413	.977	.00394
12	10,310	29.00	7,210	.00402	.977	.00384
13	1,450	14.00	1,020	.01310	.977	.01260
14	4,680	17.42	3,260	.00534	.977	.00511
15	6,830	23.90	4,770	.00500	.977	.00478
16	21,440	51.10	14,910	.00342	.977	.00326
17	44,700	87.80	31,100	.00282	.977	.00269
18	53,500	101.00	37,150	.00272	.977	.00259
19	62,700	110.60	43,600	.00254	.977	.00241
20	73,200	120.50	50,800	.00237	.977	.00226
21	14,300	42.40	9,980	.00425	.977	.00406
22	17,230	43.60	12,020	.00363	.977	.00346
23	90,100	141.00	62,700	.00225	.977	.00215
24	102,400	164.10	71,300	.00230	.977	.00220
25	104,300	153.30	72,600	.00211	.977	.00199
26	115,800	174.50	80,500	.00217	.977	.00206
27	121,000	153.20	84,300	.00182	.977	.00173
28	127,600	174.00	88,900	.00196	.977	.00187
29	130,000	155.40	90,500	.00172	.977	.00164
30	135,900	183.30	94,500	.00194	.977	.00184
31	133,500	195.80	93,200	.00210	.977	.00201
32	120,200	162.00	83,800	.00193	.977	.00183
33	112,800	142.70	78,300	.00182	.977	.00173
34	97,800	144.50	68,000	.00213	.977	.00202
35	88,900	134.00	61,750	.00217	.977	.00206
36	78,200	122.00	54,450	0.00225	0.977	0.00213

TABLE XIII

LOCAL HEAT TRANSFER COEFFICIENT
IN EACH SECTION

Test No.	1	5	10	13	16	18
Section						
13	51.3	68.5	67.7	64.0	69.0	95.3
12	7.8	8.6	9.0	7.9	15.1	22.9
11	2.9	4.4	6.0	2.5	8.4	17.5
10	3.2	5.1	6.7	3.3	8.0	17.1
9	2.4	3.9	4.7	2.3	8.1	13.2
8	2.1	3.3	5.1	2.0	7.7	13.3
7	2.2	3.6	4.9	1.9	7.6	14.4
6	1.8	3.0	5.0	1.9	5.7	14.3
5	1.4	2.4	3.4	1.4	5.9	11.2
4	1.1	2.8	3.4	1.5	4.9	12.7
3	0.8	2.3	2.6	1.2	4.8	12.5
2		2.0	3.2		5.4	10.6
1	3.2	5.4	8.1	4.5	8.3	14.8

Test No.	20	24	26	31	34	36
Section						
13	80.0	98.0	87.0	102.0	103.2	104.2
12	26.0	35.6	31.8	37.3	31.0	31.0
11	19.9	28.1	26.1	31.6	24.7	24.2
10	16.6	26.9	26.3	27.8	26.4	22.8
9	16.9	25.3	26.9	27.3	26.1	22.9
8	15.4	24.9	28.1	29.2	25.4	21.8
7	15.4	22.7	22.8	24.9	22.7	20.0
6	14.9	20.4	23.5	25.3	23.1	19.9
5	13.7	18.2	18.6	21.2	18.6	17.1
4	14.3	19.2	24.2	24.8	21.7	18.8
3	12.9	18.6	19.7	23.2	19.2	17.9
2	12.1	17.6	18.9	22.1	17.0	14.9
1	15.3	18.7	21.8	22.6	18.9	18.0

TABLE XIV

PECLET NUMBERS

Test No.		1	5	13
N_{Re} N_{Pr}		1,660	3,792	1,020
Section	x/D	$\frac{x}{D}$	$\frac{1}{N_{Re}\ N_{Pr}}$	x 10^3
13	0.534	0.32	0.14	0.43
12	1.068	0.64	0.28	0.85
11	2.136	1.28	0.56	1.71
10	3.200	1.92	0.84	2.56
9	4.790	2.88	1.26	3.83
8	6.40	3.84	1.68	5.10
7	8.26	4.95	2.18	6.60
6	10.40	6.23	2.74	8.16
5	13.05	7.84	3.44	10.40
4	15.75	9.45	4.15	12.60
3	18.45	11.01	4.86	14.70
2	21.65	13.00	5.70	17.30
1	25.10	15.10	6.60	20.00

Test No.		10	18	20	31
N_{Re} N_{Pr}		10,100	37,150	50,800	93,200
Section	x/D	$\frac{x}{D}$	$\frac{1}{N_{Re}\ N_{Pr}}$	x 10^4	
13	0.534	0.534	0.144	0.105	0.057
12	1.068	1.056	0.288	0.210	0.114
11	2.136	2.101	0.577	0.420	0.228
10	3.200	3.160	0.863	0.629	0.343
9	4.790	4.730	1.29	0.943	0.512
8	6.40	6.350	1.73	1.26	0.685
7	8.26	8.180	2.23	1.63	0.884
6	10.40	10.30	2.81	2.05	1.110
5	13.05	12.91	3.53	2.57	1.400
4	15.75	15.60	4.26	3.10	1.680
3	18.45	18.27	4.98	3.64	1.970
2	21.65	21.40	5.87	4.27	2.320
1	25.10	24.90	6.78	4.94	2.690

TABLE XV

LOCAL NUSSELT NUMBER
IN EACH SECTION

Test No.	1	5	10	13	16	18
Section						
13	458.0	688.0	602.0	572.0	615.0	844.0
12	70.0	76.6	80.8	71.7	134.6	204.0
11	26.6	39.6	54.6	22.5	76.0	156.3
10	29.2	47.0	61.0	30.3	72.7	152.5
9	22.3	35.7	43.2	21.2	73.9	118.0
8	20.4	30.8	46.1	19.4	70.3	120.0
7	21.4	34.4	44.5	19.0	69.7	130.0
6	17.4	28.5	46.2	18.4	52.6	128.9
5	14.0	22.8	31.6	13.5	54.8	102.1
4	10.6	27.4	31.3	15.3	45.5	116.5
3	8.1	22.4	24.6	12.7	45.0	114.9
2		20.0	30.2		51.0	97.5
1	32.0	53.2	78.0	48.0	79.3	137.0

Test No.	20	24	26	31	34	36
Section						
13	709.0	869.0	772.0	903.0	908.0	929.0
12	232.0	317.0	283.0	333.0	275.0	276.0
11	177.5	250.0	233.0	284.0	220.0	218.0
10	148.5	241.0	236.0	249.0	237.0	205.0
9	151.7	227.0	232.0	245.0	234.0	206.5
8	139.0	224.5	254.0	264.0	230.0	196.0
7	139.0	205.0	203.0	224.5	205.0	181.5
6	134.3	184.0	212.0	228.0	210.0	180.0
5	125.0	166.0	170.0	193.5	168.5	156.0
4	131.1	176.1	222.0	227.0	198.0	171.5
3	118.5	170.6	180.6	213.0	175.0	164.5
2	111.0	161.5	173.5	203.0	156.0	137.0
1	141.1	172.5	201.0	209.0	173.6	166.5

TABLE XVI

DATA FOR LAMINAR FLOW RANGE

Test No.	N_{Pe}	N_{Nu}	$(D/L)^{1/3}$	$(\mu_b/\mu_w)^{0.14}$	$\frac{N_{Nu}}{(D/L)^{1/3}(\mu_b/\mu_w)^{0.14}}$
1	1,660	13.70	0.341	1.018	39.70
2	2,438	14.50	0.341	1.019	41.80
3	822	8.13	0.341	1.016	23.45
4	2,695	15.90	0.341	1.019	46.00
13	1,020	14.00	0.341	1.015	40.50

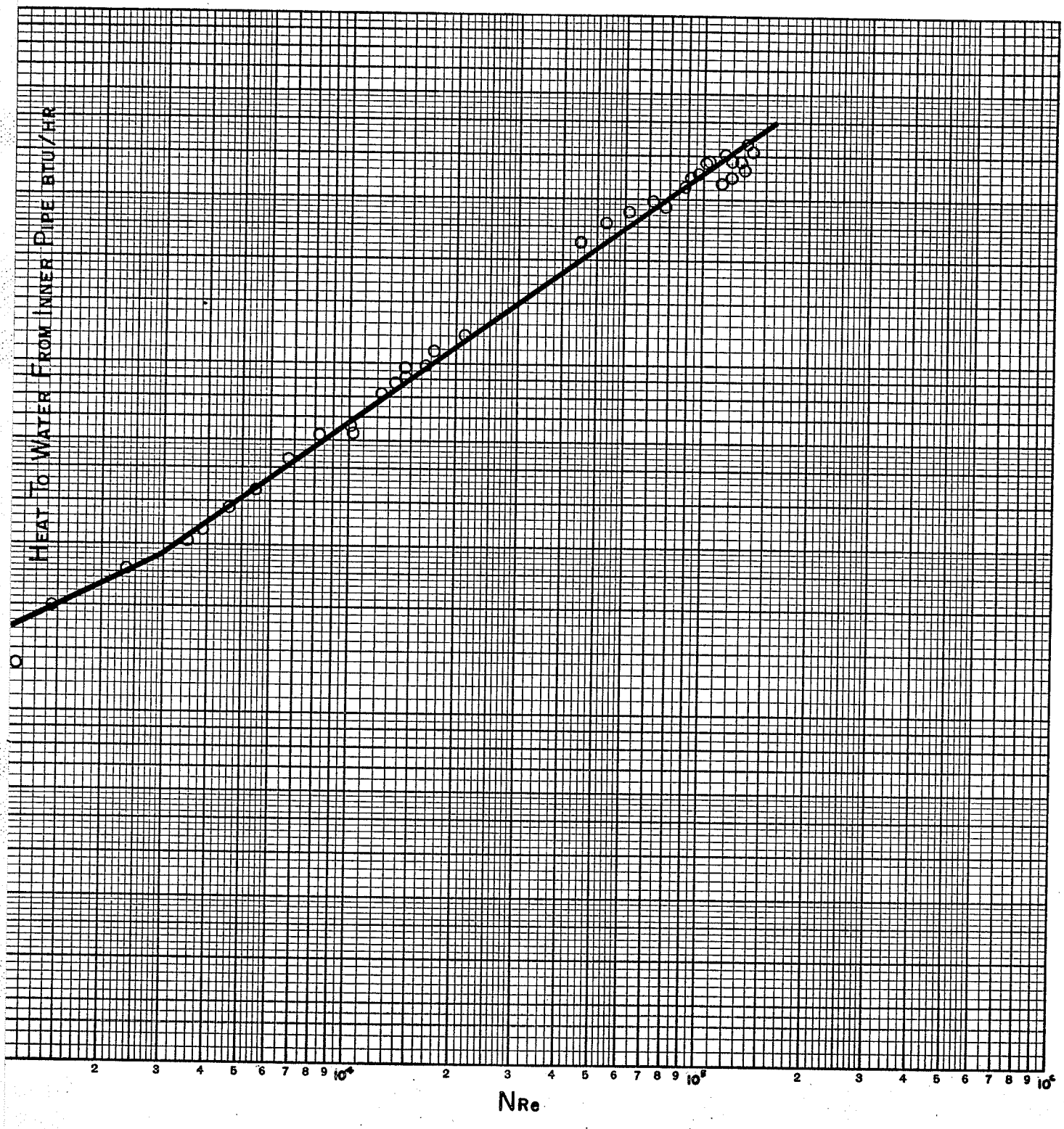

FIGURE 15

VARIATION OF HEAT TRANSFER WITH REYNOLDS NUMBER

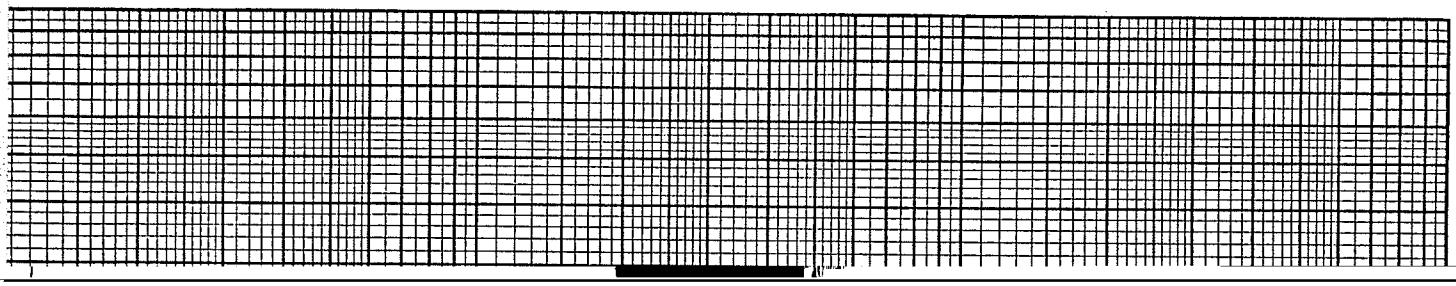

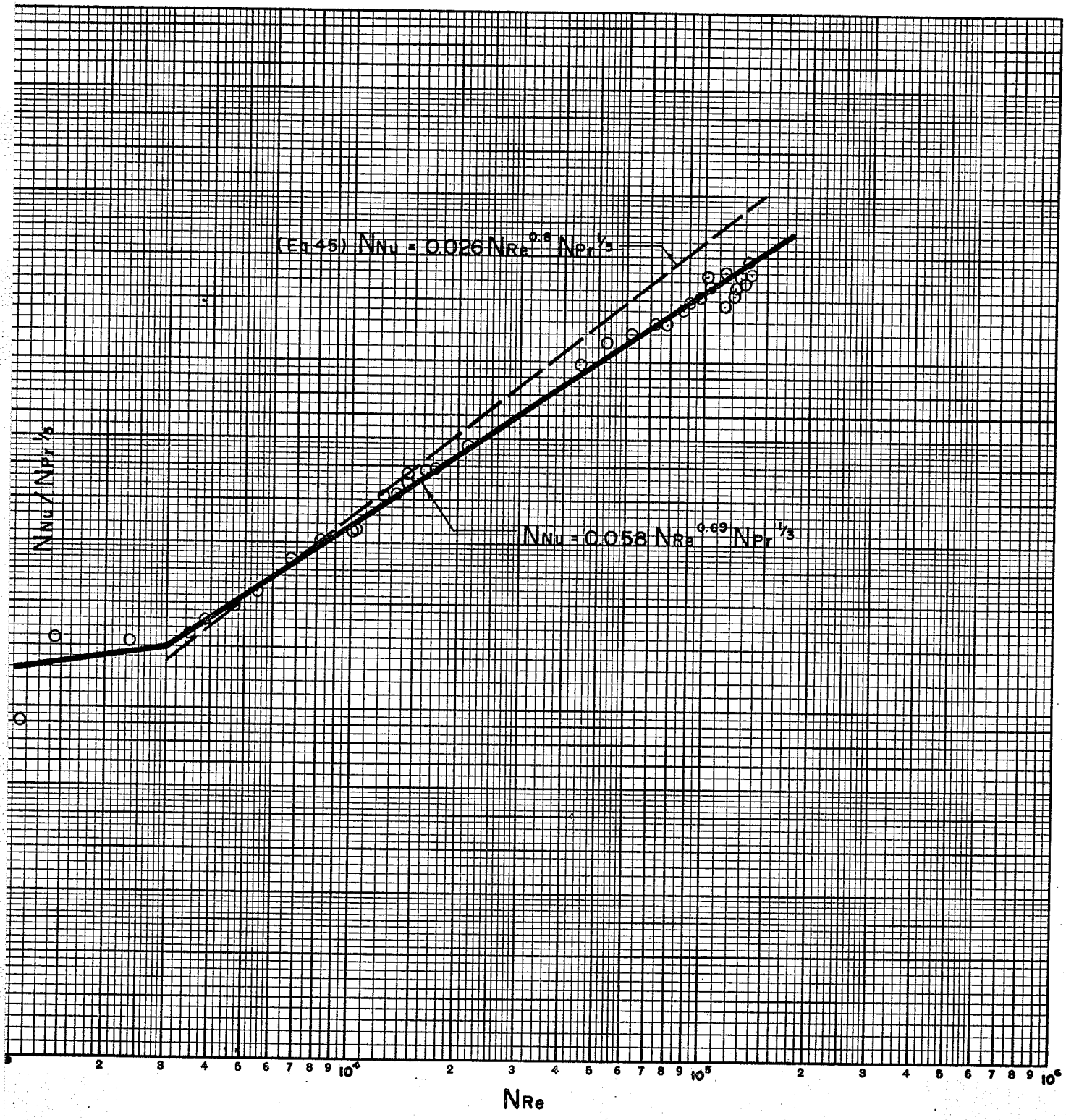

FIGURE 17

VARIATION OF $N_{Nu} / N_{Pr}^{1/3}$ WITH REYNOLDS NUMBER

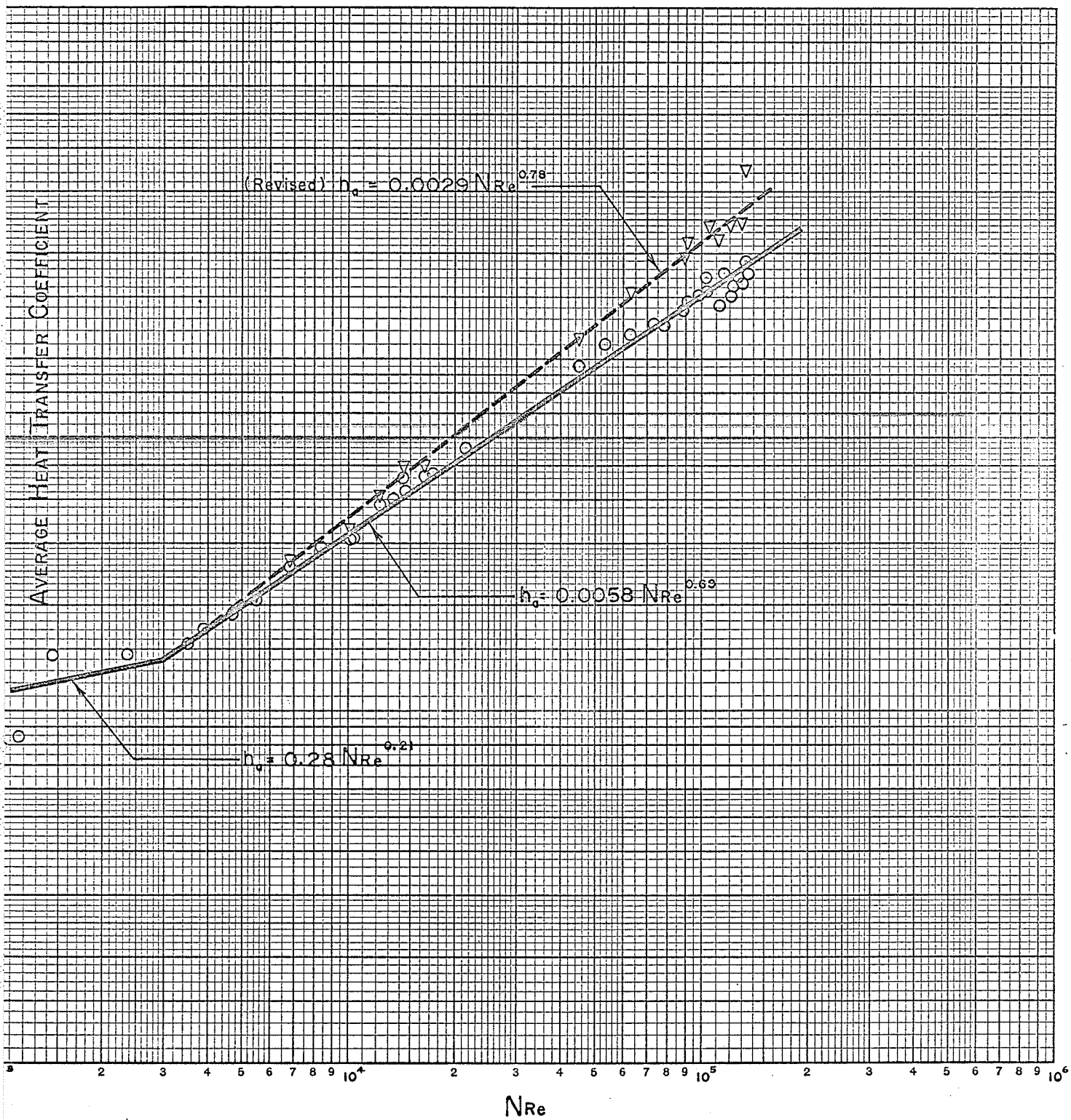

FIGURE 18

VARIATION OF THE AVERAGE HEAT TRANSFER COEFFICIENT WITH REYNOLDS NUMBER

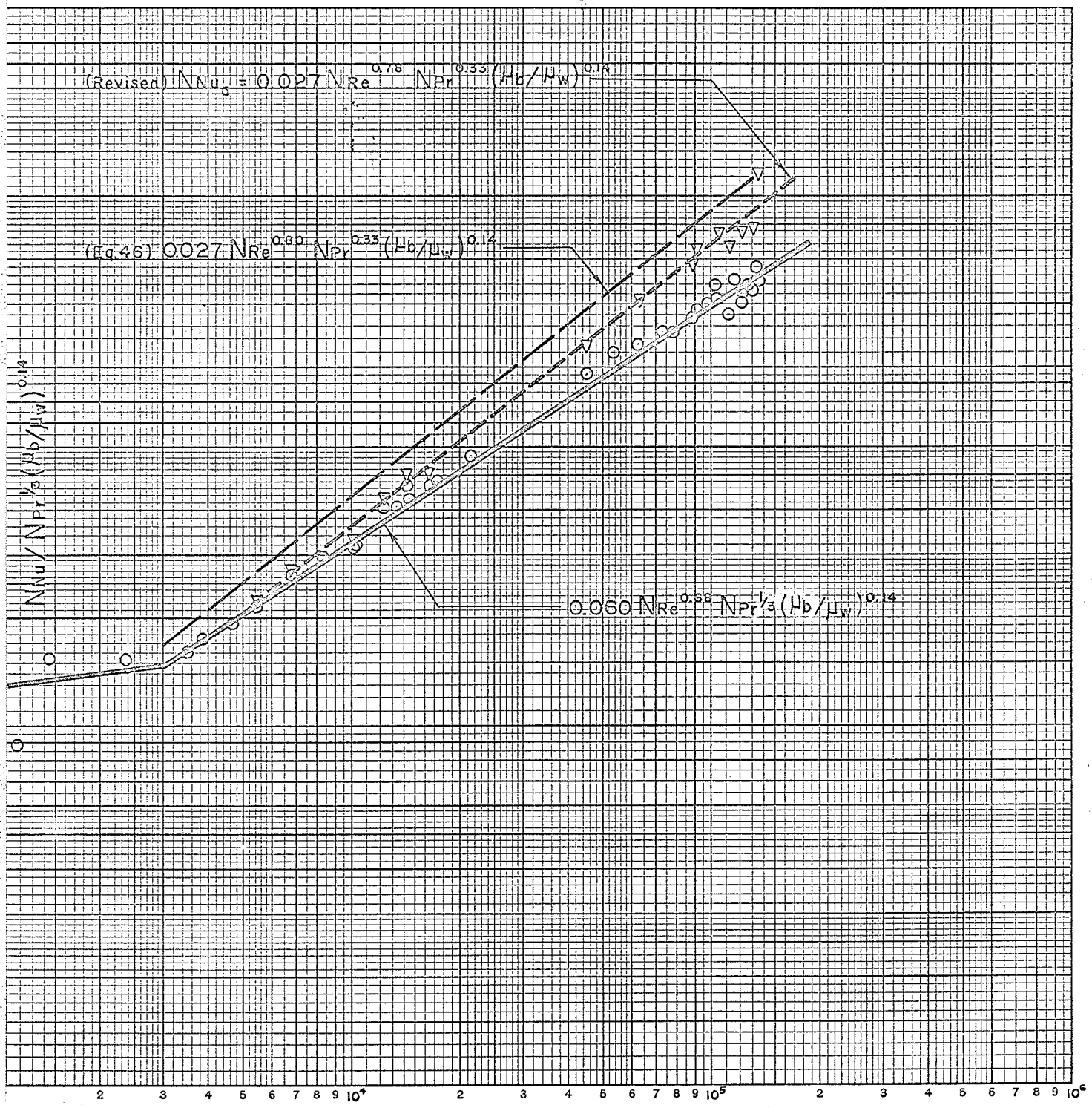

FIGURE 19

VARIATION OF $N_{Nu}/N_{Pr}^{1/3}(\mu_b/\mu_w)^{0.14}$ WITH REYNOLDS NUMBER

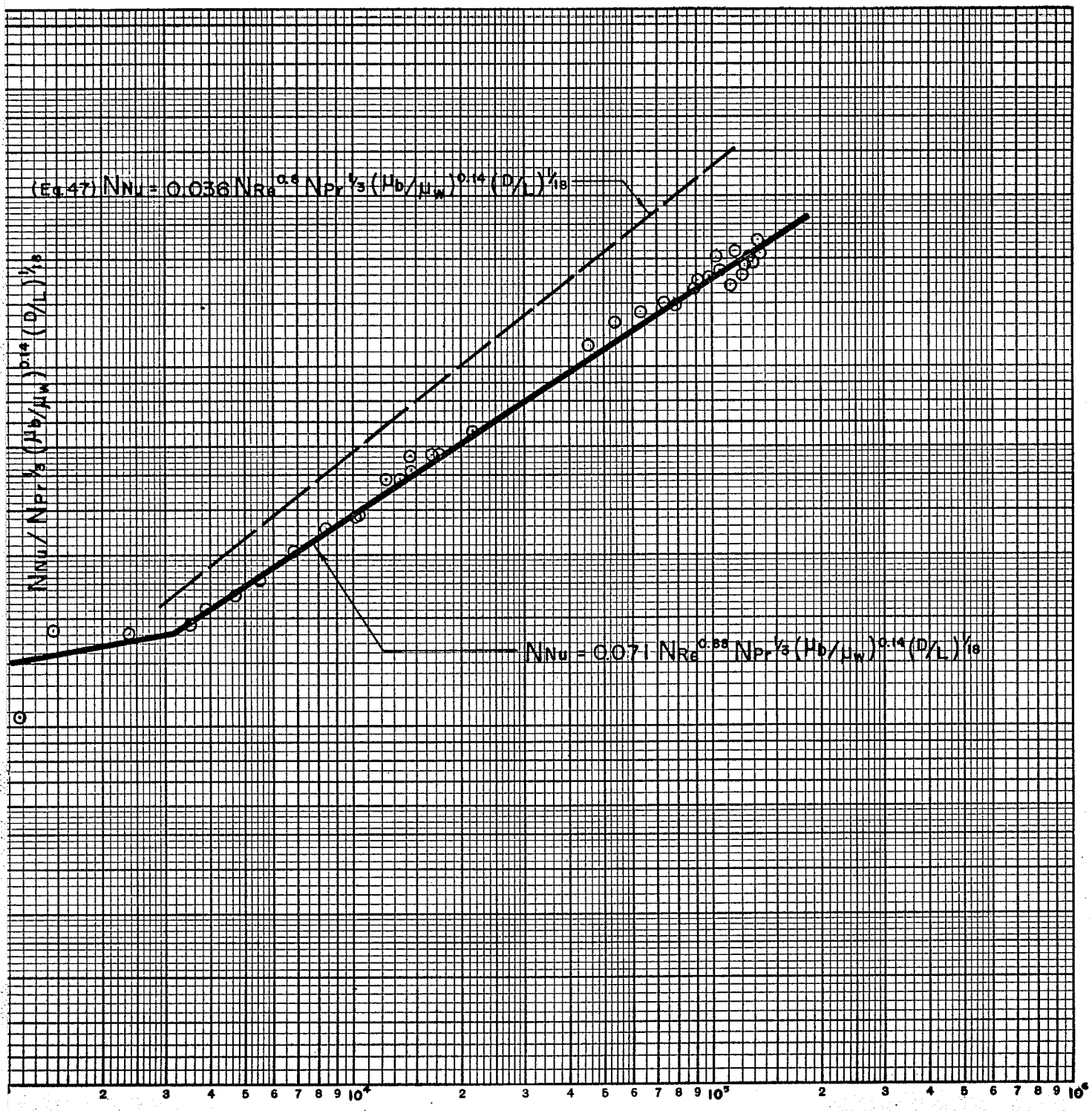

FIGURE 20

VARIATION OF $N_{Nu}/N_{Pr}^{1/3} (\mu_b/\mu_w)^{0.14} (D/L)^{1/18}$ WITH REYNOLDS NUMBER

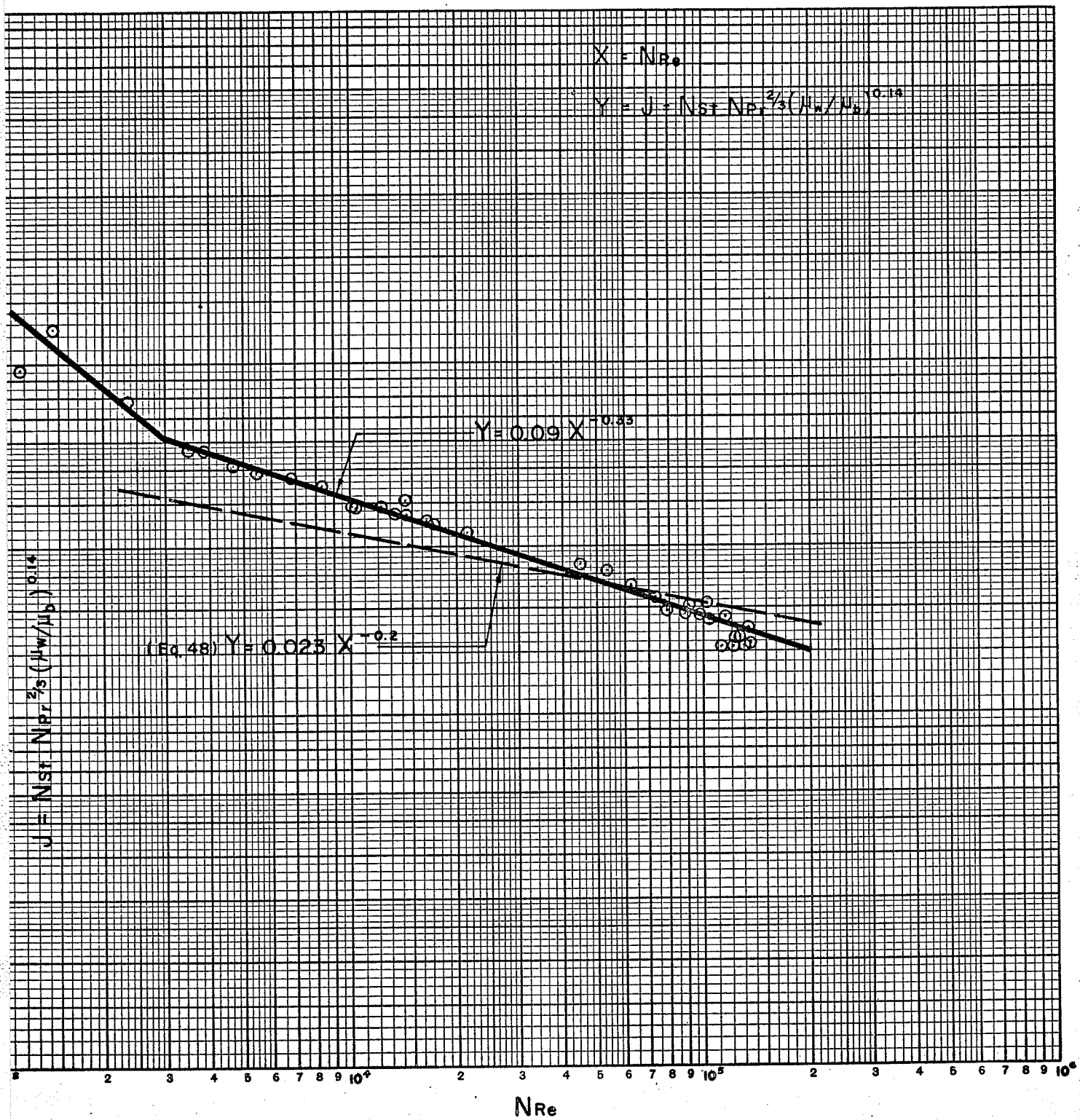

FIGURE 21

VARIATION OF $N_{St}\, N_{Pr}^{2/3} (\mu_w/\mu_b)^{0.14}$ WITH REYNOLDS NUMBER

FIGURE 22

VARIATION OF THE LOCAL HEAT TRANSFER COEFFICIENT ALONG THE TUBE LENGTH

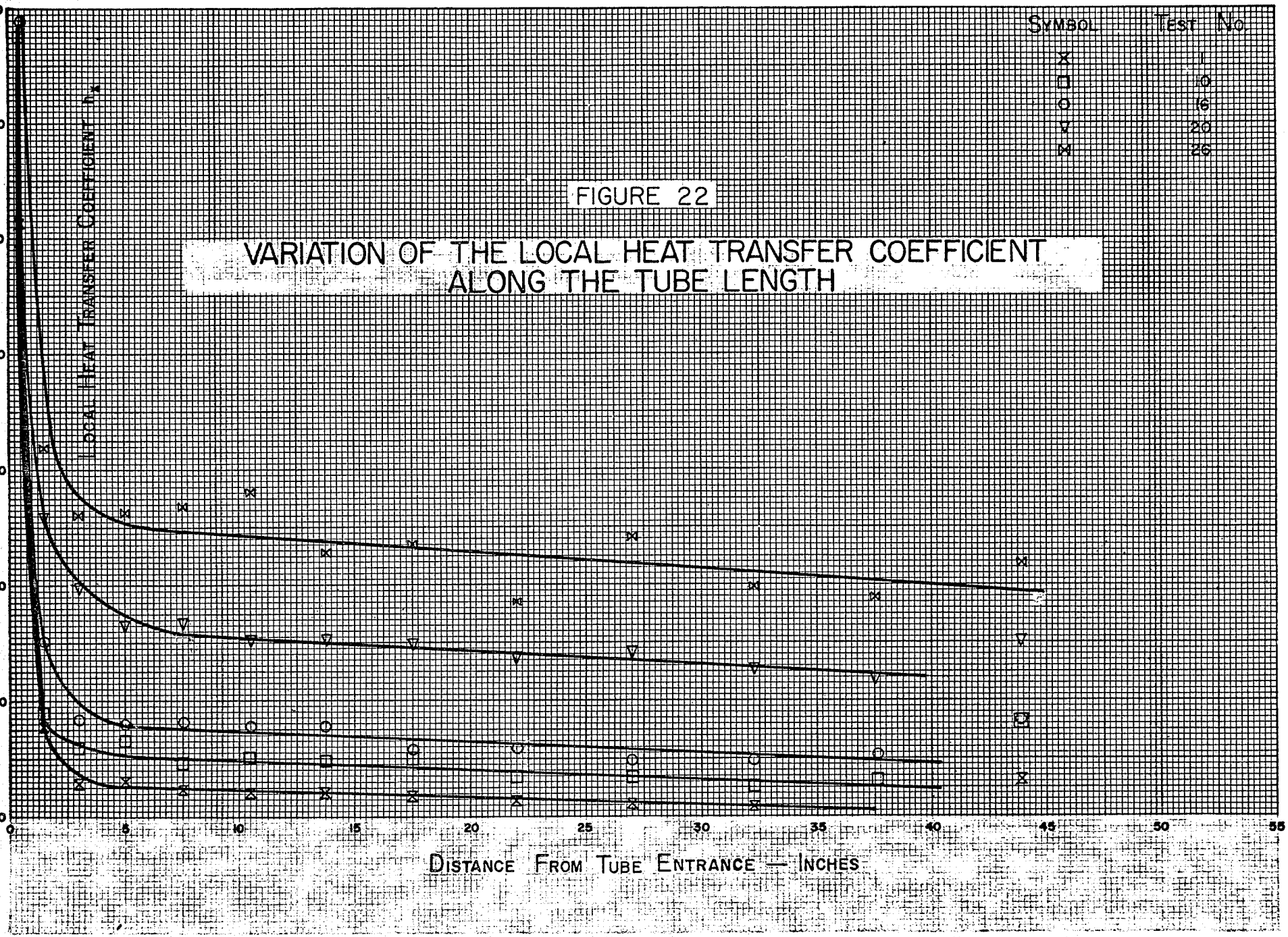

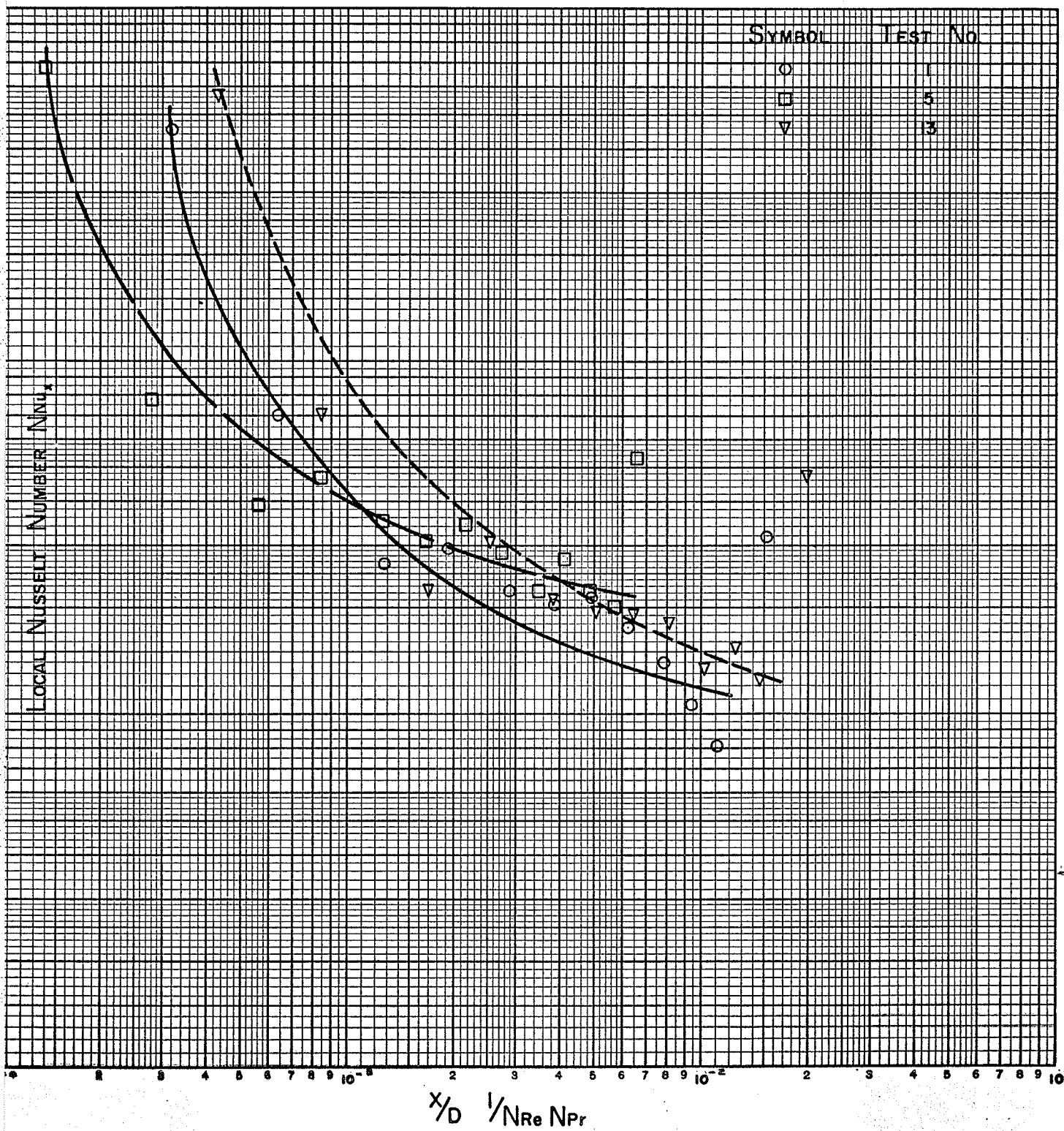

FIGURE 23

EFFECT OF DISTANCE FROM TUBE INLET ON LOCAL NUSSELT NUMBER

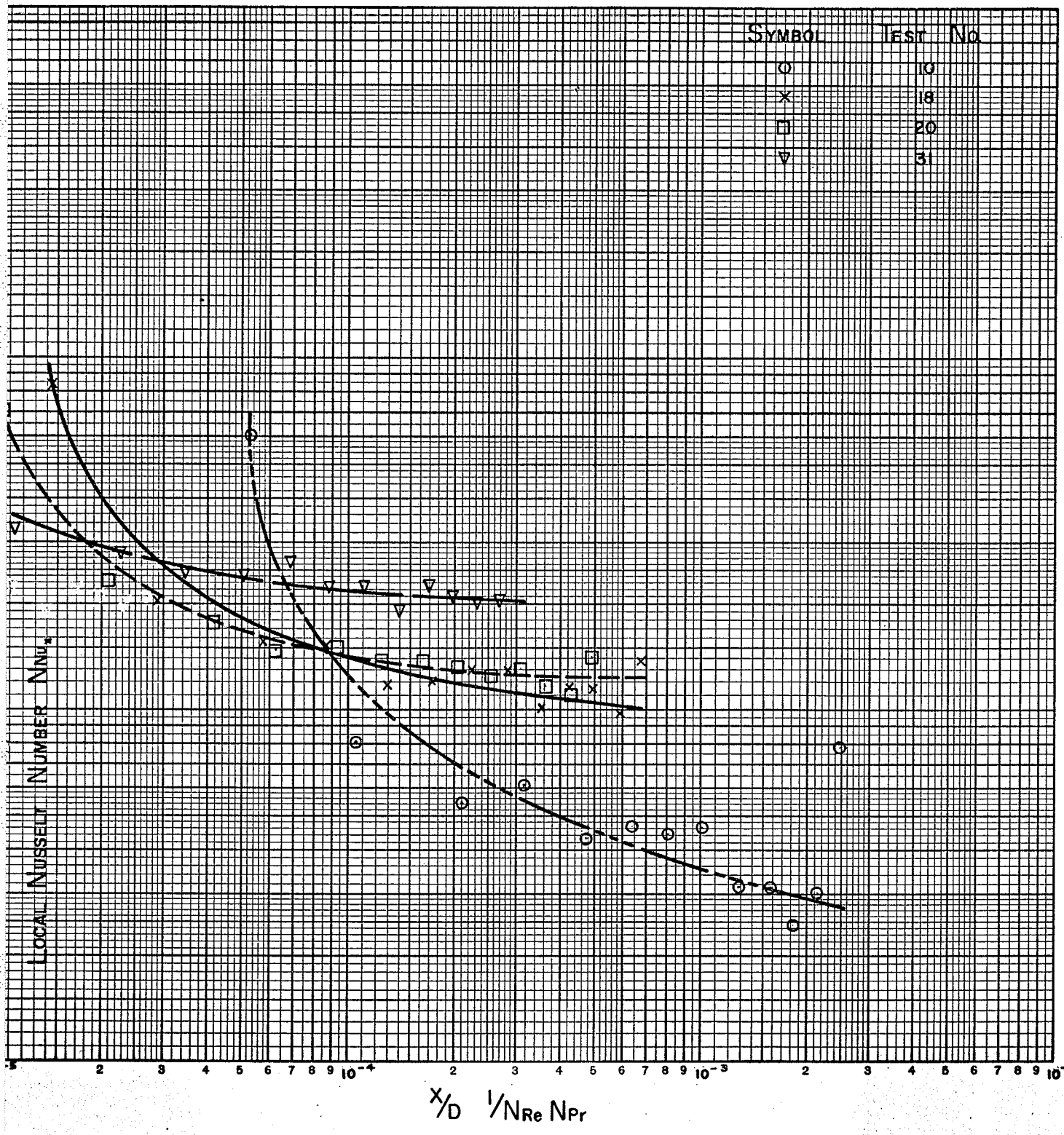

FIGURE 24

EFFECT OF DISTANCE FROM TUBE INLET ON LOCAL NUSSELT NUMBER

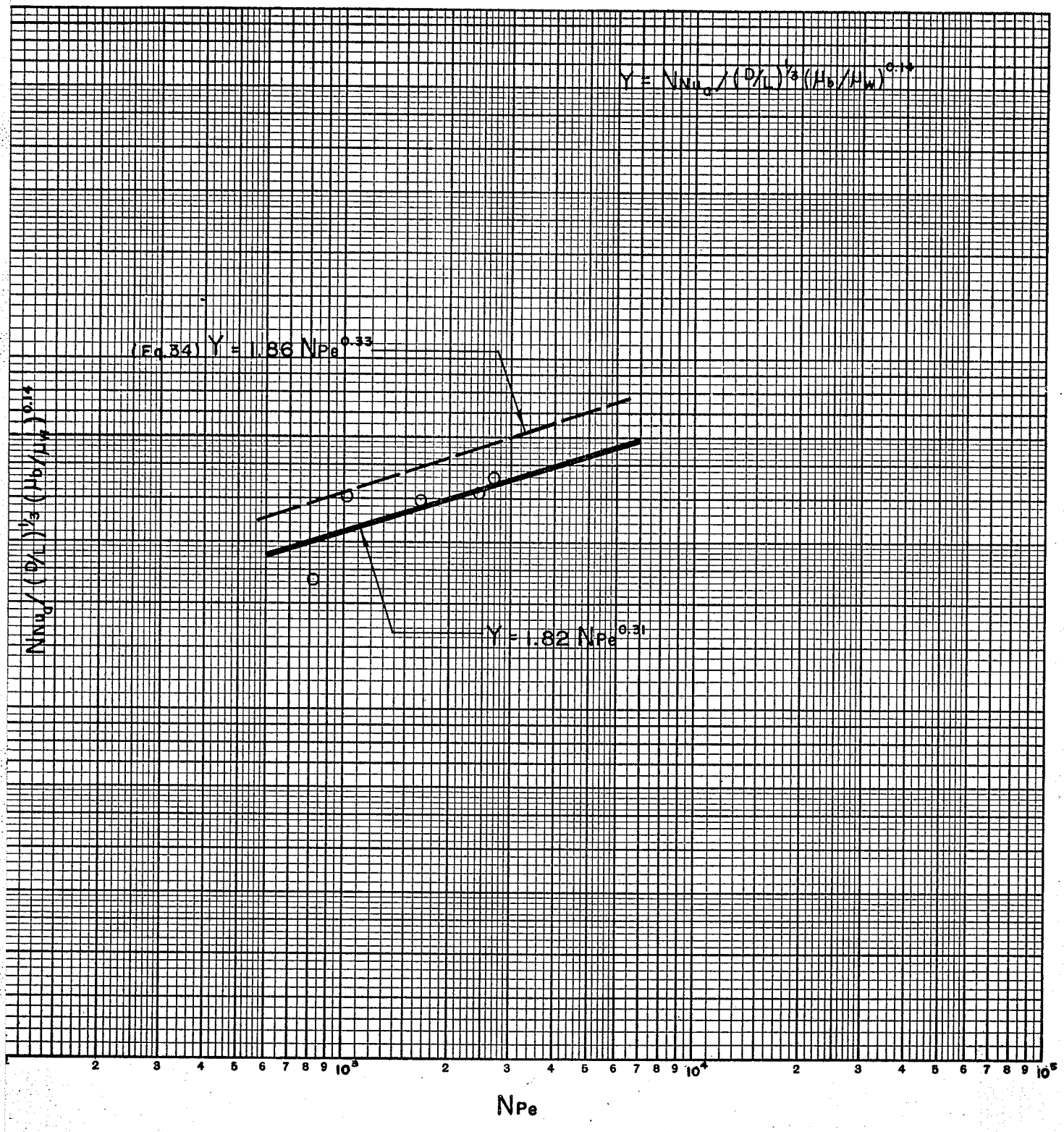

FIGURE 25

VARIATION OF $N_{Nu}/(D/L)^{1/3}(\mu_b/\mu_w)^{0.14}$ WITH PECLET NUMBER FOR LAMINAR FLOW CONDITIONS

ERROR ANALYSES

SAMPLE CALCULATION

1. Mass Flow W.

For test #23

Variations in successive readings of h_v at the same point of the impact tube traverse were such that h_v varied from 2.705 to 2.795 for position #8 in the traverse, i.e. variation = .09/2.70 x 100 = 3.3%

For position #10 = .06/2.02 x 100 = 2.9%

Possible error in mass flow measurement ± 3.0%

2. Heat Gained by Water

Temperature Rise

Test #5 temperature rise = 5.3°F

reading accuracy = 0.1°F

% error = 0.1/5.3 x 100 = 1.9% say 2%

Water Flow

Test #5 Water collected per bucket - approximately 10 lbs.

reading accuracy .01 lbs.

% error = .01/10 x 100 = 0.1% (negligible)

Possible error in heat gained by water ± 2%

3. Heat Loss by Air in Inner Pipe

Error in temperature drop through test section consists of

error in inlet temperature plus error in discharge temperature.

Error in Inlet Temperature:

Test #5

$$\text{Inlet temperature} = t_t + \frac{t_j + t_b}{2} \Big/ 2$$

where t_t = tank temperature = 175.7°F

t_j = jacket temperature = 180.0°F

t_b = by-pass temperature = 180.3°F

$(t_j + t_b)/2 = 180.15°F$

Therefore error = (180.15 - 175.7)/2 = 2.2°F

Temperature drop through test section (Table V) = 55.5°F

% error = 2.2/55.5 x 100 = ± 4.0%

Test #35

$(t_j + t_b)/2 = 183.5$

$t_t = 177.5$

Therefore error = (183.5 - 177.5)/2 = 3.0°F

Temperature drop through test section (Table V) = 25.7°F

% error = 3.0/25.7 = ± 11.7%

Error in Discharge Temperature:

Reading error ± 0.5°F

Test #5, temperature drop through test section = 55.5°F

Therefore % error = 0.5/55.5 x 100 = 0.9%

Test #35, temperature drop = 25.7°F

% error = 0.5/25.7 x 100 = 1.9%

Error Due to Temperature Measurement Being Made a Short Length After the Test Section:

For test #16

$$\frac{3}{47.125} \times \frac{4.5}{5.6} \times \frac{20}{113.6} \times 100 = 0.90\%$$

where 3/47.125 = ratio of lengths

$\frac{4.5}{5.6}$ = $\frac{\text{local } h_x \text{ at end of section}}{\text{average } h_a \text{ for test section}}$ (Figure 22)

20/113.6 = ratio of temperature difference to jacket vs. annulus

For test #26

$$\frac{3}{47.125} \times \frac{18}{19.35} \times \frac{20}{121.6} \times 100 = 0.97\% \text{ say } 1\%$$

Total possible error in discharge temperature reading =

1.9% + 1.0 = 2.9%

Adding this to possible error in inlet temperature yields a total possible error in temperature drop of 11.7 + 2.9 = 14.6%

Combining with possible error in mass flow measurement, yields an error in heat loss by air of:

1.03 x 114.6 = 118.0 = ±18%

4. Heat Gained from Surroundings

The error in heat gained from surroundings consists of sum of errors in air and water heat gain or loss:

2 + 18 = 20%

5. L. M. T. D.

For test #5

Maximum error in inlet air temperature = 2.2°F

Maximum error in outlet water temperature = 0.1°F

Maximum error in outlet air temperature:

= 2.9% x temperature drop

= 0.029 x 55.5 = 1.6°F

Maximum error in inlet water temperature = 0.1°F

Consequently, calculation for L. M. T. D. would yield

$$\text{L. M. T. D.} = \frac{(177.9+2.2) - (44.1-0.1) - (122.4+1.6) - (38.8+0.1)}{\text{Ln} \quad \Delta T \text{ hot}/\Delta T \text{ cold}}$$

$$= \frac{(180.1 - 44.0) - (124.0 - 38.9)}{\text{Ln } 136.1/85.1}$$

$$= \frac{51.0}{0.47} = 108.8^{\circ}\text{F}$$

Note: this is within 2° of calculated value

Therefore % error in L. M. T. D. = 1.8%

6. Average Overall Heat Transfer Coefficient U_a

This is a product of the error in the calculation of heat from air and the L. M. T. D.

i. e. 118.0 x 101.8 = 120.0

i. e. Maximum possible error = 20%

7. Average Heat Transfer Coefficient h_a

As h_a is calculated from the relation

$$\frac{1}{h_a} = \frac{1}{U_a} - \text{(factor dependent on } h_w\text{)}$$

h_a varies directly as U_a providing $\frac{1}{U_a}$ is large compared to the factor due to h_w.

for $h_w = 400$ and test #31

check effect on h_a if U_a is increased by 20%

$$\frac{1}{h_a} = \frac{1}{20.40 \times 1.2} - .0029 = 0.0379$$

$$h_a = 25.8$$

$$25.8/21.7 \times 100 = 119\%$$

Consequently h_a is also subject to 20% error.

For test #31 at $h_w = 100$

$$\frac{1}{h_a} = \frac{1}{20.40 \times 1.2} - .0104 = .0304$$

$$h_a = 32.9$$

This is $32.9/25.9 \times 100 = 127\%$

Therefore a 20% error in U_a results in a 27% error in h_a.

8. Calculation of U_s to Surroundings

The area used in the calculation of U_s should have included the water supply header and the individual supply lines, consequently the area should have been 6.13 ft^2 in lieu of 3.69ft^2. The values of U_s would thus be only 60% of the values tabulated in Table VI.

The value of U_s is subject to the same error as the heat gained from surroundings calculated in item 4 as 20%.

9. Prandtl Number

Error negligible as data read directly from published data.

10. Average Nusselt Number

Subject to same errors as h_a calculated in item 7.

11. Local Heat Transfer Coefficient

Error in calculation of ΔT, includes error in heat from surroundings (20%) and error in mass flow (3%).

Therefore error = 1.20 x 1.03 = 1.23 i.e. 23%

U is calculated from heat by water (error 2%) less heat from surroundings (error 20%)

Therefore error in U = 2 + 20 = 22%

Error in h_x, as noted in item 7 is dependent on error of U and assumed value of h_w.

Comparison of Calculated Heat Gain From Surroundings Using Published Data for U_s

From McAdams[5], the combined free convection and radiation loss or gain from room to pipe corresponding to a temperature difference of $40^{\circ}F$ is 1.84 BTU/hr/ft^2/$^{\circ}F$.

The test accuracy can be verified by checking heat balance across the test section, to obtain heat from surroundings, using

an area of 6.13 ft^2 (see item 8).

Test #1

Heat from surroundings from test results = 450 BTU/hr

From published data = 1.84 x 6.13 x 32.4 = 365 BTU/hr

This is 365/450.0 x 100 = 81.2% of calculated.

Test #5

From test results = 465.8 BTU/hr

From published data = 1.84 x 6.13 x 36.8 = 414 BTU/hr

Accuracy = 414/465.8 x 100 = 88.0%

Test #16

From test results = 520.0 BTU/hr

From published data = 1.84 x 6.13 x 40.3 = 455.0 BTU/hr

Accuracy = 455.0/520.0 x 100 = 87.5%

Test #24

From test results = 420.0 BTU/hr

From published data = 1.84 x 6.13 x 32.6 = 368.0 BTU/hr

Accuracy = 368.0/420.0 x 100 = 87.5%

Test #34

From test results = 640.0 BTU/hr

From published data = 1.84 x 6.13 x 36.6 = 412 BTU/hr

Accuracy = 412/640 x 100 = 64.3%

Effect of h_w of 50 on calculated value of h_a

Further to sample calculation item 7.

Test #1

$$\frac{1}{h_a} = \frac{1}{U_a} - \left(\frac{1}{50} + .0004\right)$$

$$= \frac{1}{1.45} - .0204 = 0.6646$$

$$h_a = 1.49$$

This is only 2% higher than when h_w assumed as 500.

Test #19

$$\frac{1}{h_a} = \frac{1}{11.60} - 0.0204 = 0.0645$$

$$h_a = 15.50$$

This is 26.9% higher than when h_w assumed as 500.

Test #31

$$\frac{1}{h_a} = \frac{1}{20.40} - 0.0204 = .0286$$

$$h_a = 35.0$$

This is 61.1% higher than when h_w assumed as 500.

Check on Correct Range for h_w

By Natural Convection

Using an alignment chart from McAdams[5].

Temperature difference between water in annulus and inner pipe for test #31 = $122^{\circ}F$

$$\frac{P^2 \Delta T}{D} = \frac{1 \times 122}{1.93} = 63.3$$

where P = pressure in atmospheres= 1

ΔT = temperature difference = $122^{\circ}F$

D = diameter of inner pipe = 1.93"

from alignment chart $h_w = 35$

Using Relation by McAdams for Flow of Liquids Normal to a Horizontal Cylinder.

$$Y = 0.35 + 0.56\, X^{0.52}$$

where $X = \frac{DVP}{\mu}$ $\quad Y = \frac{h_w\, D/K}{(C_p\, \mu/K)^{0.3}}$

D = outside diameter of inner pipe = 0.061 ft.

ρ = $= 62.5$ lbs/ft^3

μ = at $45^{\circ}F$ $= 3.73$ lbs/hr/ft

V = velocity in annulus

K = at $45^{\circ}F$ $= 0.324$

C_p = $= 1$

Check velocity through section 6 for test #30

Area of annulus for section 6 = 0.0431 ft^2

Water flow = 16.50 lbs/20 min. = 0.825 lbs/min.

= 0.0132 ft^3/min

Velocity = .0132/.0431 = 0.307 ft/min = 18.4 ft/hr

$X = \frac{0.161 \times 18.4 \times 62.5}{3.73} = 49.7$

$Y = 0.35 + 0.56 \times 49.7^{0.52}$

$= 4.61$

Solving for h_w yields

$$h_w = \frac{4.61 \times (1 \times 3.73/.324)^{0.3} \times 0.324}{0.161}$$

$$h_w = \underline{19.3}$$

It follows that a value of h_w in the range of 50 or less should have been used in the calculations.